Investigations on the action mode of *Bacillus thuringiensis* Cyt2Aa1 toxin

by

Mohamed S. Abdel Rahman

A thesis
presented to the University of Waterloo
in fulfillment of the
thesis requirement for the degree of
Doctor of Philosophy
in
Biology

Waterloo, Ontario, Canada, 2015

Author's Declaration

I hereby declare that I am the sole author of this thesis. This is a true copy of the thesis, including any required final revisions, as accepted by my examiners.

I understand that my thesis may be made electronically available to the public.

Abstract

B. thuringiensis is a Gram-positive bacterium that, while quite otherwise closely related to the soil saprophyte *Bacillus cereus*, is unique in producing a large variety of membrane-damaging, insecticidal protein toxins. These toxins, which are widely used as biopesticides, fall into two major structural families, named Cry and Cyt. This thesis reports experiments that characterize the activity and membrane specificity of Cyt2Aa1 toxin, which is a member of the Cyt family. This toxin is shown to have a low degree of antibacterial activity against Gram-positive bacteria; the growth of the model organism *Bacillus megaterium* is inhibited in the presence of approximately 700 μg/mL of the toxin. The toxin readily binds to the bacterial cell surface, and marker release experiments show that the bactericidal effect arises through permeabilization of the bacterial membrane. In contrast, the Gram-negative organism *E. coli* is not inhibited by Cyt2Aa1, and the toxin fails to bind to the bacterial cells.

Furthermore, it is shown that the cytolytic activity of the toxin is inhibited by cholesterol. The extent of inhibition is greater on model liposomes, in which virtually complete suppression is observed above a molar fraction of 20% or greater of cholesterol, than with red blood cells that were subjected to partial cholesterol extraction with methyl-β-cyclodextrin. Since cholesterol inhibits rather than activates Cyt2Aa1, its absence from bacterial membranes does not account for the low susceptibility of bacterial cells to the toxin.

In previous studies, two different mechanisms have been proposed for the permeabilization of membranes by Cyt2Aa1, namely, the formation of discrete, oligomeric transmembrane pores, and the diffuse disruption of the target membrane in a detergent-like manner. A series of experiments that used both wild-type toxin and several point mutants

with impaired hemolytic activity provides evidence for the formation of toxin oligomers that precedes the permeabilization of the target membrane. Moreover, osmotic protection experiments with polyethyleneglycol suggest the formation of pores with limited, but possibly heterogeneous size. Collectively, these findings support the notion that Cyt2Aa1 acts through the formation of discrete oligomeric pores.

Acknowledgements

First and foremost, I would like to express my deepest thanks to my supervisor Dr. Michael Palmer, a humble scholar, true gentleman, and inspiring adviser. I am deeply grateful and thankful for the chance of working in his research group. Without his patience, continuous encouragement, knowledgeable guidance and persistent support, this thesis would have not been possible. His support and sense of humour have made the entire experience a complete enjoyment.

I would also like to thank my advisory committee members, Drs. Bernard R. Glick and J. Guy Guillemette for their valuable suggestions and comments. Furthermore, I would like to thank Drs. Bae-Yeun Ha and Stefan Siemann for serving as examiners of my thesis.

I am also very appreciative for all the help from these fantastic colleges: Dr. Jawad Muraih, Dr. TianHua Zhang, Eric Brefo-Mensah, Dr. Lisa Pokrajac, Brad Scott, and Robert Taylor.

To all my friends from the chemistry and biology departments, thank you for all the encouragement, help, and the great times, which will be always remembered.

And to all the administrative staff members, thank you for all your help throughout the years.

Dedication

To my family

Contents

List of Figures

List of Tables

List of Abbreviations

Bt	*Bacillus thuringiensis*
Cry	Crystal insecticidal proteins of Bt
Cyt	Cytolytic insecticidal proteins of Bt
DMPC	1,2-dimyristoyl-sn-glycerol-3-phosphocholine
DMPG	1,2-dimyristoyl-sn-glycero-3-phosphoglycerol
EM	Electron microscopy
HBS	HEPES Buffer Saline
HEPES	4-(2-Hydroxyethyl)piperazine-1-ethanesulfonic acid
IPTG	Isopropyl-β-D-thiogalactopyranoside
LB	Luria-Bertani broth
OD	Optical density
PBS	Phosphate-buffered saline
PC	Phosphatidylcholine
PFT	Pore-forming Toxin(s)
PMSF	Phenylmethanesulfonyl fluoride
SDS	Sodium dodecylsulfate
SDS-PAGE	Sodium dodecylsulfate polyacrylamide gel electrophoresis
TBS	Tris-buffered saline
VIP	vegetative insecticidal protein of Bt
WT	wild type

Chapter 1

Introduction

This thesis deals with a specific protein toxin, Cyt2Aa1, of the Gram-positive, endospore-forming bacterium *Bacillus thuringiensis* (*B. thuringiensis*; *Bt*). Cyt2Aa1 belongs to one of two major families of δ-endotoxins, which are expressed by *B. thuringiensis* during sporulation, and both of which have powerful insecticidal activity. Toxin-enriched preparations of *B. thuringiensis* cultures are widely used in agriculture for crop protection. Because of their economic significance, *Bt* toxins have attracted considerable research interest. While much has been learned about their molecular modes of action, many open questions remain. Before discussing the particular questions that were addressed in this thesis (see Section 1.4), I will first give an overview of the previous work on *B. thuringiensis* and its insecticidal toxins.

1.1 *Bacillus thuringiensis*

In 1901, the soil bacterium *Bacillus thuringiensis* was discovered in Japan by S. Ishawata, who also reported that this bacterium killed

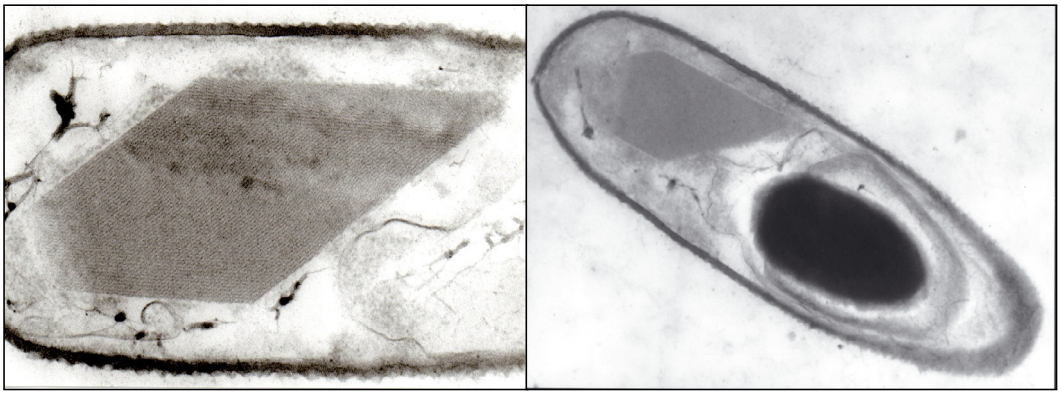

Figure 1.1 Transmission electron micrographs of longitudinal sections of *B. thuringiensis* cells. Adapted from [5]. Left: a parasporal crystal shown at high magnification. These protein crystals contain the δ-toxins. Right: entire cell with endospore and parasporal crystal.

Bombyx mori, the silkworm [1]. Subsequently, in 1911, E. Berliner identified *B. thuringiensis* as a pathogen of the caterpillars of Mediterranean flour moths, in which the bacterium causes a disease known in German as "Schlafsucht" (hypersomnia, that is, excessive sleep). Berliner had isolated his specimen in the German province of Thuringia [2], which gave rise to the bacterial species name. Soon after, Berliner also discovered the inclusion bodies that form concomitantly with the endospore (see Figure 1.1). In 1953, Hannay and Fitz-James reported that these inclusion bodies consist of proteins and named them "parasporal crystals" [3]. This discovery marks an important milestone in the development of *B. thuringiensis* as a biopesticide [4].

The first commercial biopesticide consisting of sporulated *B. thuringiensis* cultures was produced in France in 1938; this preparation was used to control flour moths. In 1961, *Bt*-based biopesticides were approved for use in the United States by the U.S. Environmental Protection Agency. For approximately 20 years, various crop plants have been genetically engineered to express *Bt* toxins. Such insect-resistant transgenic crops provide an effective and inexpensive means for

pest control, allowing for a significant reduction in the use of chemical insecticides [6].

B. thuringiensis, like all *Bacillus* species, is aerobic; it is non-capsulated and motile with peritrichous flagella. The species comprises numerous subspecies or strains, each of which produces its own unique combination of insecticidal δ-toxins, expressed within the parasporal crystals during sporulation. Thus far, several thousand natural *B. thuringiensis* strains have been isolated from diverse sources like soil, plants and insects [7]. Examples of such strains are the subspecies *kurstaki* [8], *aizawai* [9], *galleriae* [10], which was found to be active against lepidopterans, as well as subsp. *israelensis* [11], *tenebrionis* [12], *kyushuensis*, and *Berliner* [13].

Classification of *B. thuringiensis* strains has been carried out using antisera to the strain-specific flagellar antigen (H serotyping) [14, 15]. At present, more than 70 H-serotypes and 82 serovars have been distinguished [14]. These serotypes and serovars can also be discriminated based on 16S rRNA, gyrB and aroE gene sequence analyses [16].

B. thuringiensis shares common phenotypic and genotypic characteristics with *Bacillus anthracis* and *Bacillus cereus*, and together they are placed into the *Bacillus cereus* (BC) group [17]. Recently, there has been some controversial discussion as to whether or not *B. thuringiensis* should be regarded as a species separate from *B. cereus* and *B. anthracis*. Whether or not it we consider it a species, the formation of the insecticidal parasporal is a specific feature that sets it apart from *B. cereus* and *B. anthracis* [18].

1.1.1 The life cycle of *B. thuringiensis*

The life cycle of *B. thuringiensis* starts from the vegetative form of the bacteria. Under typical culture conditions, it takes approximately 13 hours for the vegetative form to complete the process of sporulation. This process occurs in successive stages, which are illustrated in Figure 1.2. At the outset (stage 0 in the figure), the growing vegetative cell

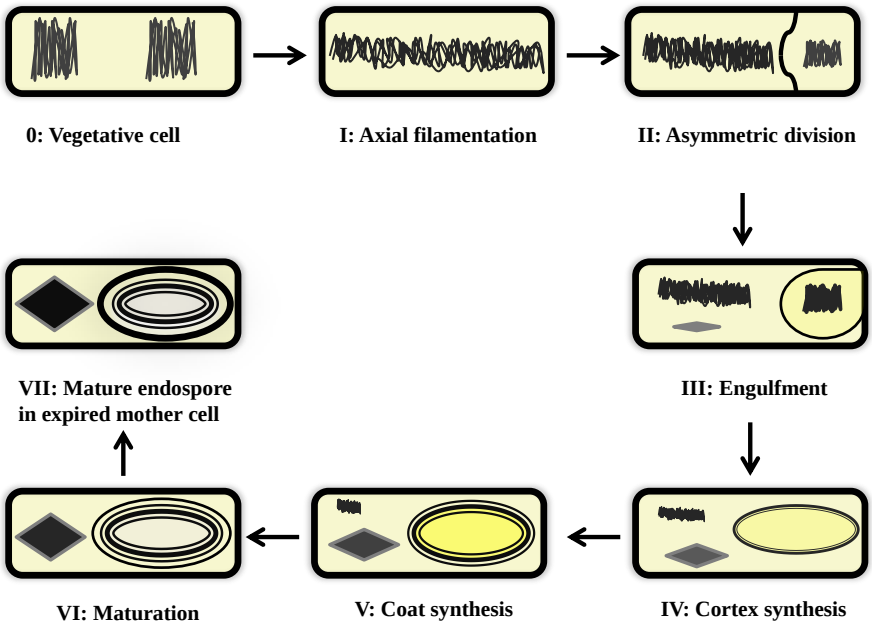

Figure 1.2 Schematic representation of the stages of *Bacillus thuringiensis* spore formation. The rhomboid shapes represent the parasporal crystals that contain the *Bt* toxins. The various stages are explained in the text.

has completed DNA replication and thus contains two complete chromosomes. The cell undergoes the following morphological changes [19–21]:

(I) The two chromosomes, which still hang together, form a stretched axial filament across the cell.

(II) A membranous division septum is formed that asymmetrically divides the cell into a large mother cell and a smaller prespore.

(III) After seven hours overall, the prespore is engulfed by the mother cell and exists as a free-floating forespore within the mother cell. At this stage, the formation of the parasporal crystal begins.

(IV) After eight hours, the forespore is enveloped by a distinctive form of peptidoglycan, which differentiates into two layers, the primordial cell wall and the cortex.

(V) Two more protective proteinaceous layers, the spore coat and the exosporium, are deposited around the prespore.

(VI) The spore is dehydrated and develops into a mature spore with its characteristic thermal and chemical resistance properties. This process occurs without morphological changes but is accompanied by increased brightness in phase contrast microscopy.

(VII) Finally, formation of the parasporal crystals is completed. At this stage, the mother cell has lost its viability.

Unlike other *Bacillus* species, the *Bt* mother cell does not undergo lysis after sporulation is completed, and both the endospore and the parasporal crystal remain inside the mother cell. The last three stages take 3–4 hours to complete.

1.1.2 *B. thuringiensis* toxins and insecticidal activity

The insecticidal protein toxins of *B. thuringiensis* fall into three structural families, namely, the Cry, the Cyt, and the Vip families [22]. The acronym "Vip" stands for "vegetative insecticidal proteins," indicating that these toxins are expressed in the vegetative growth phase. The acronyms "Cry" and "Cyt" are abbreviations for the characteristics "crystalline" and "cytolytic", respectively [23]. Note, however, that both the Cry and the Cyt toxins are expressed within the parasporal crystals in the sporulation phase [24], and moreover that both are cytolytic (see below).

Commercial powdered preparations of *B. thuringiensis* that are used as pesticides for crop protection contain the crystals, along with spores [25]. A more recent strategy for the protection of crops such as cotton and maize is the recombinant expression of various *Bt* δ-endotoxins in the crop plants themselves, which renders them toxic to the feeding

insects. The *Bt* toxins are expressed in insoluble form, but they dissolve and undergo proteolytic activation in the alkaline milieu of the insect gut. Although at least some toxins are harmful to experimental animals when applied parenterally, they are not toxic to them when applied orally, since they are rapidly destroyed in the acidic milieu of the stomach [26].

While individual *Bt* toxins vary in activity against different insect groups and species, collectively they affect many species from the orders of Diptera (mosquitoes and flies), Lepidoptera (moths and butterflies), and Coleoptera (weevils and beetles) [27]. Moreover, the toxins affect the orders of Hymenoptera (wasps and bees); and in addition to insects, they also affect nematodes [28].

With both Cry and Cyt toxins, the most likely mechanism of membrane damage is the formation of discrete pores, although other mechanism have been proposed. This will be discussed in more detail in Section 1.3, following a brief general introduction to cytolytic proteins and peptides.

1.2 CYTOLYTIC PROTEINS AND PEPTIDES

Cytolytic or membrane-damaging proteins and peptides are exceedingly widespread in nature. They occur as toxins in bacteria and fungi, as components of insect poisons, as effector molecules in the specific and non-specific immune system, and within the repertoire of digestive mechanisms of amoeba.

The mechanism of membrane damage can be chemical, as is the case with phospholipases such as *Clostridium perfringens* α-toxin; more commonly, however, it consists in the physical disruption of membrane continuity. Here, we can further distinguish two major mechanisms. Larger protein molecules typically form discrete pores, which can often be directly observed with morphological methods such as electron microscopy. In most cases, these pores consists of oligomeric assemblies

Table 1.1 Examples of cytolytic proteins and peptides.

Type	Name	Host organisms	Target cells or organisms
proteins	complement	mammals	bacteria, viruses
	perforin	mammals	mammalian cells (self)
	α-hemolysin	*Staphylococcus aureus*	mammalian cells
	δ-endotoxins	*B. thuringiensis*	insect larvae
	colicin IA	*E. coli*	*E. coli* (different strains)
peptides	defensins	mammals	bacteria, fungi
	melittin	Honey bee	mammalian cells
	alamethicin	fungi (*Trichoderma viride*)	fungi and bacteria
	amoebapore	*Entamoeba histolytica*	bacteria

of the toxin molecules. In some cases, the oligomers are sufficiently stable to allow their purification and crystallization; the first such crystal structure was obtained for *Staphylococcus aureus* α-hemolysin (see Figure 1.5A and B).

Smaller peptides often operate through more a more diffuse, detergent-like mechanism, although formation of discrete pores occurs with peptides such as melittin (see Figure 1.3). Some examples of cytolytic proteins and peptides are listed in Table 1.1.

1.2.1 Bacterial pore-forming toxins

Unlike the Cry and the Cyt toxins, most other bacterial pore-forming toxins do not accumulate intracellularly but are instead secreted from the cell as water-soluble molecules.[1] Typically, they bind to their target cell membranes as monomeric molecules and then undergo oligomer-

[1] An exception is pneumolysin, formed by *Streptococcus pneumoniae*, which accumulates intracellularly in soluble form.

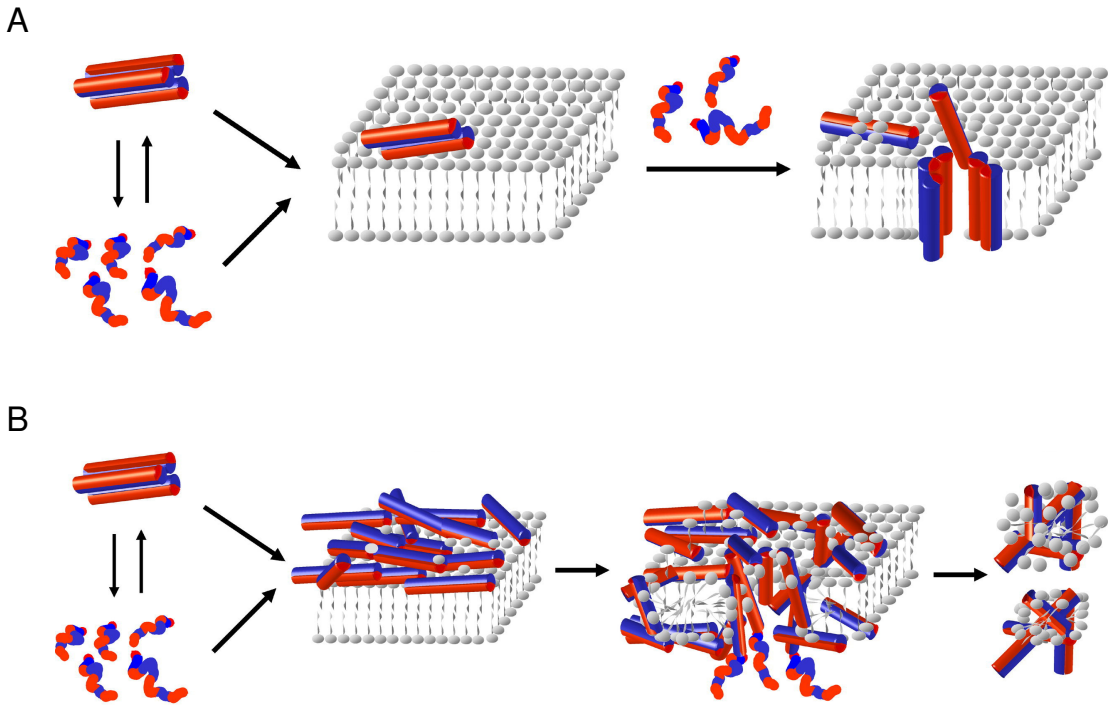

Figure 1.3 Mechanisms of membrane damage by antimicrobial peptides (adapted from [29]). A: In the "barrel stave" mechanism, amphiphilic peptides orient aggregate into clusters that orient perpendicularly to the lipid bilayers and surround discrete transmembrane pores. This mechanism is exemplified by metlittin. B: In the "carpet" or detergent-like mechanism, peptides bind and insert into the headgroup layer of the membrane. Beyond a certain threshold of peptide coverage, the curvature strain breaks up the membrane. An example of this mechanism is alamethicin.

ization, which sets the stage for membrane insertion and permeabilization. This transformation often involves extensive conformational changes [30]. Pore formation causes osmotic imbalance, loss of essential metabolites, and breakdown of ion gradients, which subsequently leads to cell swelling, lysis and death [31]. With some bacterial toxins, pore formation is not the main toxic mechanism by itself but primarily serves to translocate toxic enzymes across the membrane and into the cells; examples are diphtheria, cholera, and pertussis toxins, and also

Pseudomonas aeruginosa exotoxin (see Figure 1.4). Toxins with such a dual mode of action are collectively referred to as "A-B toxins;" they tend to have much lower lethal dosages than pure pore-formers.

Binding of the toxin molecules to the target membranes is often, but not always mediated by specific receptors. These receptors can be lipids or proteins. Cholesterol, which is not found in bacterial cell membranes (save those of mycoplasmas that live in association with animals), mediates binding of streptolysin O and homologous toxins, and also of the structurally unrelated *Vibrio cholerae* cytolysin [32].[2] Phosphocholine headgroups of phosphatidylcholine and sphingomyelin likely form the receptors for *S. aureus* α-hemolysin [33]. Cholera toxin binds to the ganglioside G_{M1}, while Shiga toxin binds to glycoproteins that bear terminal β-1,4-linked *N*-acetylglucosamine residues [34], and the glycan moieties of glycosyl-phosphatidylinositol-anchored (GPI-anchored) proteins serve as receptors for *Aeromonas hydrophila* aerolysin [35] and *Streptococcus agalactiae* CAMP factor [36].

A widely used classification of pore-forming toxins (PFTs) is based on predominant features of secondary structure [30]. The α-PFTs are mostly α-helical in structure. These toxins have pore-forming domains consisting of a three-layer structure with up to ten helices sandwiching a hydrophobic helical hairpin in the center of the structure (see Figure 1.4), which is thought to drive the initial step of the insertion process. The helical structure is retained after membrane insertion is completed. The other major class are the β-PFTs, which tend to be rich in β-sheets and insert into membranes to form a β-barrel. Representative structures of α- and β-PFTs are shown in Figures 1.4 and 1.5, respectively.

[2] This toxin is unrelated to cholera toxin; it is responsible for the hemolytic phenotype of *V. cholerae* El-Tor.

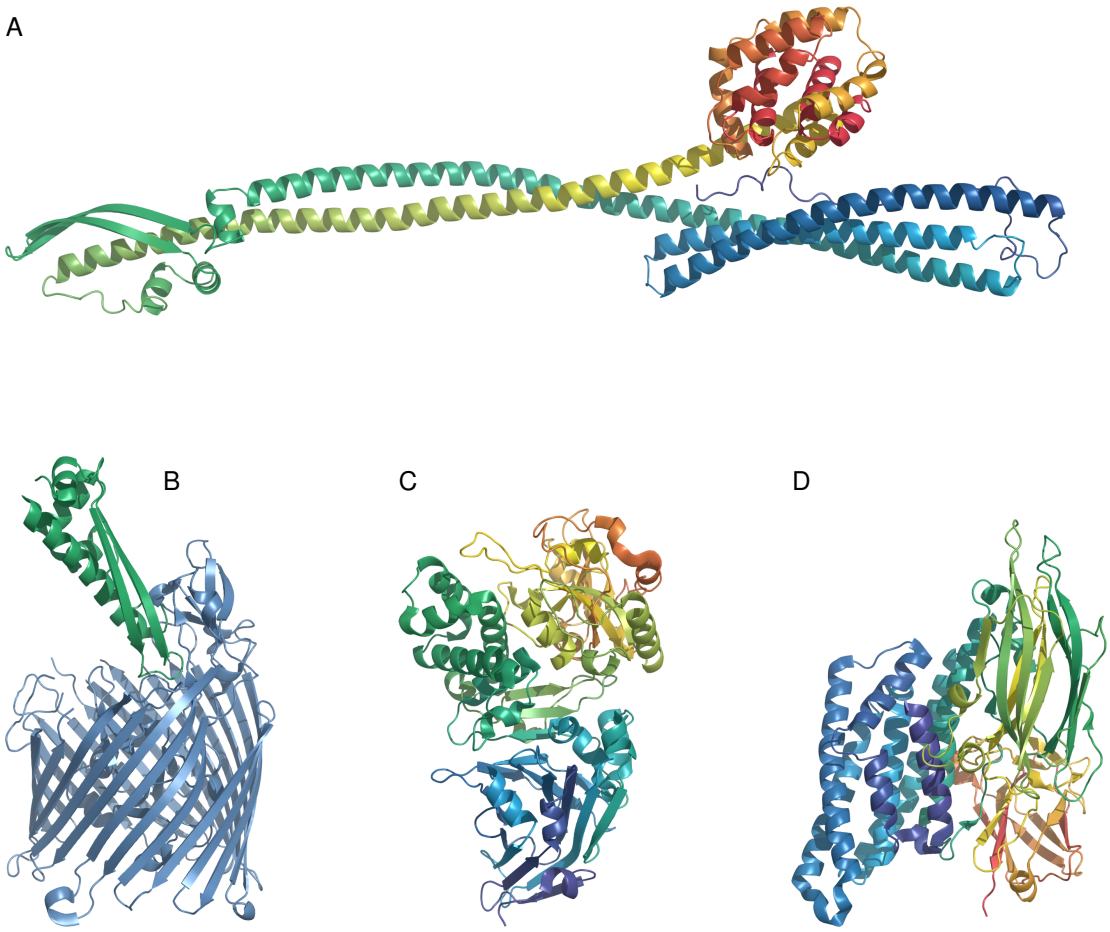

Figure 1.4 Representative α-PFT structures. Where spectral colors are used, the N-terminus is shown in blue, and the C-terminus in red. A: Colicin Ia (rendered from 1CII.pdb, [37]). B: Colicin I receptor complex (blue) with receptor binding domain of Colicin Ia (green; from 2HDI.pdb, [38]). C: *Pseudomonas aeruginosa* exotoxin (from 1IKQ.pdb, [39]). The pore-forming domain consists of the green-shaded α-helices at the top left. D: *B. thuringiensis* Cry3Bb1 insecticidal δ-endotoxin (from 1JI6.pdb, [40]).

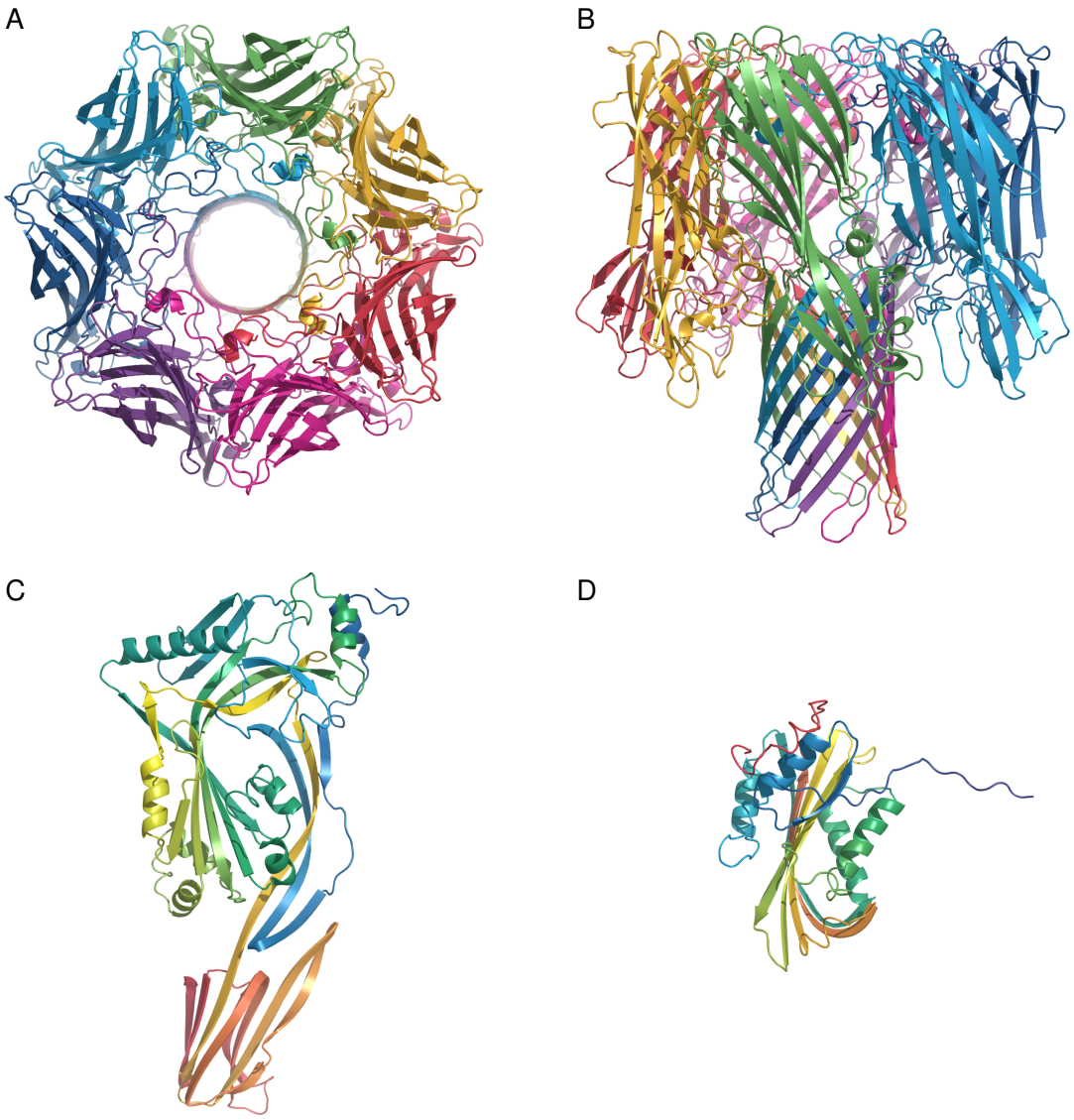

Figure 1.5 Examples of β-PFT structures. A and B: The heptameric pore formed by *Staphylococcus aureus* (rendered from α-hemolysin 7AHL.pdb, [41]). Each of the seven subunit is rendered in a different color. C: The soluble monomer of *Clostridium perfringens* perfringolysin, a cholesterol-dependent cytolysin (from 1PFO.pdb, [42]); D: *B. thuringiensis* Cyt2Aa1 δ-endotoxin monomer (from 1CBY.pdb, [43]).

1.3 STRUCTURE AND FUNCTION OF Cry AND Cyt TOXINS

While Cry and Cyt toxins differ in molecular size and predominant secondary structure (see Figure 1.4D and 1.5D, respectively), there are commonalities in their modes of action and of activation. Both are expressed as inactive protoxins, which are tightly packed inside crystalline inclusion bodies (the parasporal crystals; see Figure 1.1). These crystals are stabilized by intermolecular disulfide bridges [44] and by intramolecular salt bridges that render them insoluble at neutral pH [45]. However, the crystals dissolve at an alkaline pH of 10.5–13. The pH dependence of solubility explains why the *Bt* δ-endotoxin inclusions are toxic to insects but not humans: an alkaline pH prevails in the mid-gut juice of the insects, which contrasts with the acidic nature of the stomach juice of humans.

After solubilization, both Cry and Cyt protoxins undergo proteolytic activation, which involves the removal of a number of amino acids from both the N-terminal and the C-terminal ends. Furthermore, Cry and Cyt toxins are both considered to be pore-forming toxins, and both are assumed to form oligomeric pre-pore structures containing several monomeric activated molecules prior to membrane insertion [30]. After insertion, the resulting pores cause colloidal osmotic lysis of the cells in the mid-gut, which leads to an irreversible arrest of gut movement, and the insect stops feeding. Once the insect's digestive activity has been disrupted, the *B. thuringiensis* spores may germinate, then reach the hemolymph and cause septicemia, followed by death of the insect [46].

Cry toxins and Cyt toxins differ with respect to the requirement for macromolecular receptors. Activated Cry toxins bind to specific macromolecular receptors on the surface of the mid-gut epithelia. In contrast, no specific receptors have been described for Cyt toxins. Moreover, while the formation of discrete pores is widely assumed to be the mode of action for both Cry and Cyt toxins, for the latter an alternative, de-

tergent-like mechanism of action has also been advocated (see Section 1.3.3.2).

1.3.1 The Cry toxin family

The Cry toxins are a large family; more than two hundred members have been identified that are divided into no less than 50 subgroups, based on their amino acid sequences [28] (see Table 1.2). The number of removed amino acids is variable according to the type and nature of each δ-endotoxin. For the Cry toxins like Cry1, Cry4A and Cry4B, 3–70 amino acids are usually removed from the N-terminus during activation, while up to about half of the molecule may be removed from the C-terminus [47].

X-ray structures have been determined for the activated forms of various toxins, including Cry1Aa, Cry2Aa, Cry3Aa, Cry3Bb, Cry4Aa and Cry4Ba. While all Cry toxin share a similar overall structure composed of three domains, substantial differences are observed in detail [48] (see Figure 1.6). The toxins also show substantial differences in receptor binding specificity, as well as in spectrum and level of toxicity [23].

In all Cry toxin structures, the N-terminal domain I is composed of a central hydrophobic α5 helix, which is surrounded by six amphipathic helices to form a seven-helix bundle. This arrangement resembles that found in α-PFTs such as colicin IA (see Section 1.2.1), and accordingly this domain is assumed to have a major role in pore formation, via insertion of some or all of those helices into the cell membrane [37, 45].

Toxin binding to the receptors in the cell membranes of the gut epithelia is believed to be mediated by domains II and III [49]. Domain II consists of three anti-parallel β-sheets. It is similar in structure to various carbohydrate-binding proteins such as vitellin and the lectin jacalin. Domain III consists of a tightly packed β-sheet sandwich, and it has been proposed that this dense and compact structure is important to prevent excessive C-terminal proteolysis [45, 50].

Table 1.2 The Cry toxin family and its subgroups

Cry toxin type	Subgroups	Molecular weight (kDa)
Cry I	A(a), A(b), A(c), B–G	130–138
Cry II	A–C	69–71
Cry III	A–C	73–74
Cry IV	A–D	73–134
Cry V–IX	n/a	35–129

Activated Cry toxins bind to specific receptors on the gut epithelial cell membranes of the insect. Cry1A toxins bind to four different receptors in lepidopteran insects: a GPI-anchored alkaline phosphatase (ALP), a GPI-anchored aminopeptidase-N (APN), a cadherin-like protein (CADR), and a 270 kDa glycoconjugate [51–53].

1.3.2 The Cyt toxin family

With nine known members, the Cyt toxin family is smaller than the Cry family. The Cyt toxins fall into two major groups, Cyt1 and Cyt2 [23]. Two representative toxins, Cyt1Aa (previously CytA) and Cyt2Aa (previously CytB), share 39% sequence identity, and they consist of 249 and 259 amino acid residues, respectively, in their protoxin forms. Both also share the same tertiary structure [46] and are structurally related to a cardiotoxic pore-forming toxin called volvatoxin A2, which is produced by the straw mushroom *Volvariella volvacea* [56].

In contrast to the Cry toxins, proteolytic activation removes only small peptide fragments from both the N-terminal and the C-terminal ends; with the Cyt2Aa1 toxin, the N-terminal truncation amounts to 32 amino acid residues, and the C-terminal truncation to 15 residues [46, 57].

Each toxin consists of a single domain that comprises two outer layers of α-helical hairpins, wrapped around a β-sheet (see Figure 1.7).

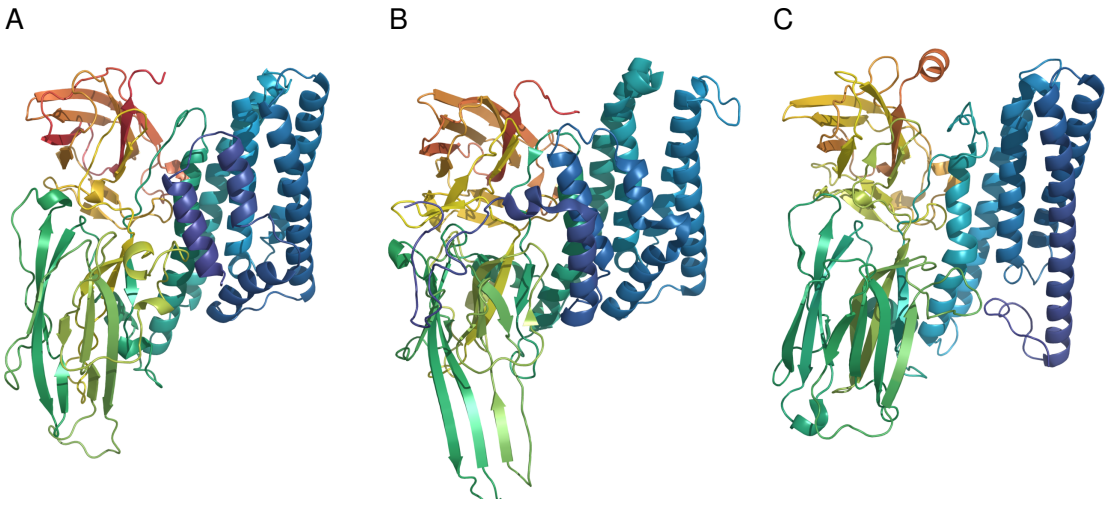

Figure 1.6 Structures of three Cry family toxins. A: Cry1Aa (rendered from 1CIY.pdb, [54]). B: Cry2Aa (from 1I5P.pdb, [55]). C: Cry4BA 1W99.pdb, [50]).

The Cyt toxins are highly specific for the larvae of dipteran insects, even though in vitro they have broad cytolytic activity against the cells from a broad range of animal species, including mammalian ones. Unlike Cry toxins, the Cyt toxins do not have any known cellular receptors, and it is assumed that these are not required for toxin activity [30]. In keeping with this assumption, they can insert into pure liposomal lipid bilayers, without any need for a protein or other macromolecular receptor [57].

While Cyt toxins are widely believed to form discrete pores, an alternative mechanism of membrane damage has been proposed [58, 59]. According to this model, Cyt toxins do not form discrete oligomeric pores but instead cause rupture of the cells by a detergent-like mode of action, similar to the mode of action of defensins and other antimicrobial peptides (see Section 1.2).

1.3.3 Cyt2Aa1 toxin

Cyt2Aa1 is a member of the Cyt family and is the specific toxin that was investigated in this thesis.

1.3.3.1 Structure. The Cyt2Aa1 toxin, previously known as CytB, is produced in vivo as a 29 kDa protoxin, which is proteolytically cleaved at both ends by gut proteases to generate the active 21–23 kDa toxin [60]. The crystal structure of the toxin in its monomeric form is composed of a single domain of $\alpha\beta$ architecture with two outer helical layers wrapped around a mixed β-sheet (see Figure 1.7). Cyt2Aa1 is produced in the protoxin form as a dimer which is cross-linked by the interlaced N-terminal strands from both monomers in a continuous, 12-stranded β-sheet (see Figure 1.7) [43, 46, 61]. Proteolytic activation by proteinase K cleaves the interlaced β-strands, removing 32 amino acid residues from the N-terminus end and 15 amino acid residues from the C-terminus to expose the three-layered core [46, 57, 61]. In contrast to Cry toxins, Cyt toxins do not bind to protein receptors but interact directly with membrane lipids [43, 57, 59].

1.3.3.2 Mode of action. Promdonkoy and coworkers characterized the interaction of Cyt2Aa1 with membranes using a cysteine mutant (L189C, in the 6^{th} strand of the central β-sheet) that was labeled with acrylodan. This fluorescent dye undergoes a pronounced emission blue-shift upon transition from a polar to an apolar environment, such as that prevailing inside lipid bilayers [62, 63]. The mutant indeed displayed a strong blue-shift upon interaction with membranes, suggesting that the labeled residue underwent membrane insertion; this was observed at both at high (37°C) and low (4°C) temperature. Aside from this single experiment, there is no detailed information on the specific residues of Cyt2Aa1 that participate in membrane interaction.

The same study also attempted to characterize the oligomeric state of Cyt2Aa1 on the target membrane; this was performed using SDS-PAGE and Western blots. Several apparent oligomeric species were observed,

A

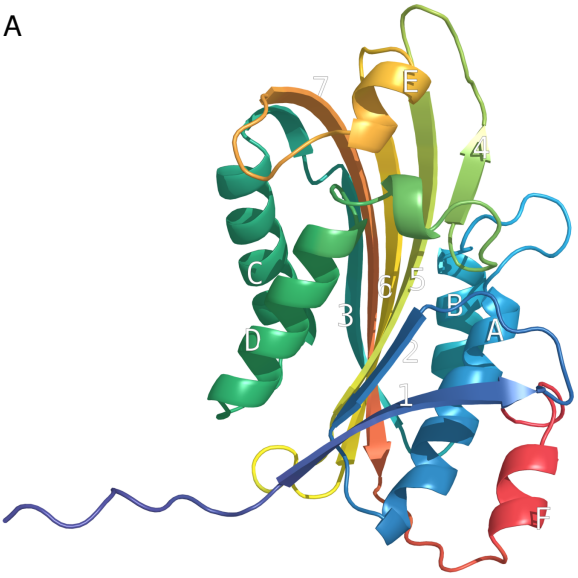

α-Helix	Residues	β-Strand	Residues
A	54–63	1	28–36
B	77–84	2	44–48
C	107–122	3	90–106
D	129–140	4	155–158
E	199–202	5	165–175
F	233–237	6	183–195
		7	210–225

B

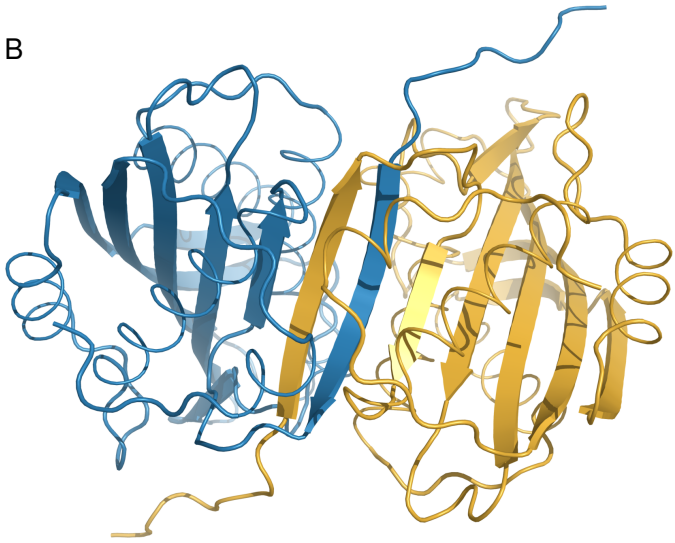

Figure 1.7 Structure of Cyt2Aa1 toxin, rendered from 1cby.pdb [43]. A: Secondary structure elements in the monomer. The labels in the structure correspond to those in the table. B: Intertwined β-sheet layers of two adjacent monomers in the crystal structure.

rather than a single one. This contrasts with observations made with *S. aureus* α-hemolysin [64] or *V. cholerae* cytolysin [65], both of which form pores with heptameric subunit stoichiometry, and it suggests that the pores formed by Cyt2Aa1 may contain variable numbers of subunits.

Discrete pores with a diameter of approximately 1 nm were characterized by Drobniewski and Ellar using both marker-release studies and osmotic protection experiments using extracellular solutes with known viscometric radii [66]. Ellar and coworkers suggested these pores to be oligomeric, consisting of an estimated six monomers [43]. This contrasts with an earlier study by Chow and coworkers [67], who extracted toxin aggregates from insect cell membranes using Triton X-100 and characterized them by density gradient centrifugation. They found a molecular mass of 400 kDa, which corresponds to a number of approximately sixteen subunits.

Knowles and coworkers have shown the permeabilization of planar lipid bilayers toward potassium after incubation with the activated toxin [68]. These authors also observed that the toxin induced the release of glucose from liposomes. They raised the question whether the cations and glucose passed through the same or through separate kinds of openings in the target membranes.

Butko and coworkers have previously performed calcein release assays with Cyt1A (Cyt1Aa1) using large unilamellar PC liposomes [69]. Calcein was released at low toxin concentration. The same authors calculated the number of toxin molecules required for the permeabilization of one liposome to be 140. From this, they concluded the formation of discrete pores to be unlikely, since in that case a single oligomer, and accordingly a much smaller number of subunits, should suffice to permeabilize a liposome. They therefore suggested a detergent-like mechanism of action.

Manceva and coworkers used fluorescence photobleaching recovery to measure the diffusion coefficient of fluorescently labelled Cyt1A and

epifluorescence microscopy to monitor the size of liposomes after incubation with Cyt1A (now calledCyt1Aa1) [59]. They found that, upon addition of Cyt1A, liposomes were broken into smaller, faster diffusing objects. They presented this as evidence of a detergent-like mode of action of the toxin, because no change in size or morphology of the liposomes is expected when discrete pores are formed.

It may be said, however, that their proposal would have more weight if the experiments had been performed with biological membranes in addition to liposomes. As it stands, the evidence in favour of pores has been reached on red cell membranes, whereas the evidence in favour of a detergent-like mode of action has been reached with liposomes. So, the mode of action might be different on both membranes.

Finally, the possibility is that the Cyt2Aa1 toxin could work by both mechanisms could be considered, because the evidence that supported both mechanisms has been obtained with high and low concentration of the toxin. So, the concentration could be the determining key to switch between both mechanisms. Another possible explanation is that both mechanisms could work with different time scale so that pores could be first formed and then disintegration of membrane by the toxin detergent-like action.

1.3.4 Antibacterial activity of *B. thuringiensis* δ-endotoxins

While the most widely known and practically important activity of the *B. thuringiensis* toxins is that against insects, both Cyt and Cry toxins have been shown to have antibacterial activity also. Expression of Cyt1Aa toxin in *E. coli* inhibits growth of the host bacterium [70]; interestingly, this can be prevented by the co-expression of two other proteins found in *B. thuringiensis* parasporal crystals (accessory proteins P19 and P20, [71]). External application of Cry4B, Cry11A and Cyt1Aa1 is toxic to *Micrococcus luteus* and several other Gram-positive species, as well as the archaeal species *Methanosarcina barkeri* [72, 73].

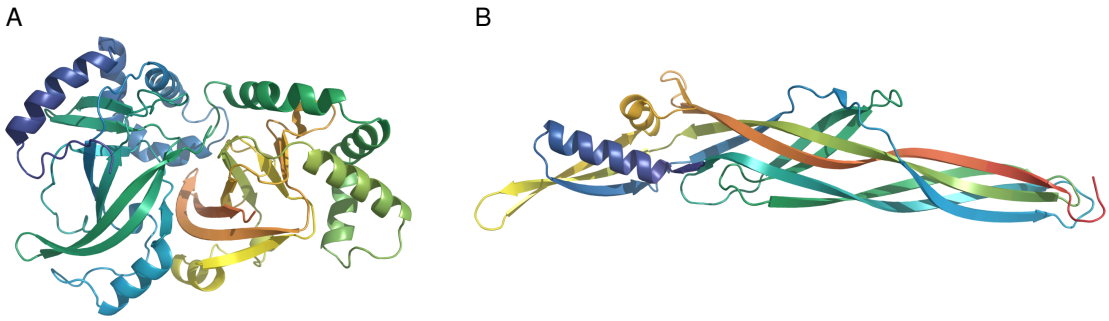

Figure 1.8 Structures of VIP toxin (A; from 1qs1.pdb) and of parasporin (B; from 2d42.pdb).

The antibacterial action of Cry and Cyt toxins have been studied by growth inhibition and by morphological methods such as electron microscopy [72–76]. While it appears likely that the mechanism of cytotoxicity is similar between bacterial and eukaryotic cells, this has not been clearly demonstrated. Moreover, the antibacterial effect of Cyt2Aa1 toxin has not been investigated so far. These questions will be addressed in Chapter 2 of this thesis.

1.3.5 Structures of other *Bt* δ-endotoxins

Bt δ-endotoxins other than Cry and Cyt include the VIP toxins (vegetative insecticidal proteins), which are produced by *Bt* vegetative cells (see Figure 1.8). These toxins have a wide spectrum of activity against lepidopteran insects [77]. Other strains of *Bt* serovar *shandongiensis* (H22) have been reported to produce a non-insecticidal toxins named parasporin [78, 79]. This toxin has no hemolytic activity but exhibits dose-dependent in vitro cytotoxicity against leukemia T cells (MOLT-4) and human uterus cervix cancer (HeLa) cells [80, 81].

1.4 AIM OF THE WORK

The tertiary structure of Cyt2Aa1 toxin is well known [43]. However, functionally, Cyt2Aa1 is one of the less well characterized toxins of

B. thuringiensis. The purpose of this study was to better characterize the mode of action of Cyt2Aa1.

Some, but not all Cyt toxins have been shown to possess antibacterial activity (see Section 1.3.4). The molecular determinants of this activity are not well understood, and it was therefore of interest to examine the antibacterial properties of Cyt2Aa1. These experiments are described in Chapter 2.

Since the results showed that Cyt2Aa1 is much less active against bacterial membranes than against mammalian membranes, the question arose whether its preference for the latter might be related to the presence of membrane cholesterol. This question was addressed with both cells (erythrocytes) and liposomes as model membranes (see Chapter 3). The outcome does not support the concept that Cyt2Aa1 requires cholesterol for activity; rather to the opposite, the sterol turned out to inhibit, not activate the toxin.

The original intention of the project described in Chapter 4 was to use cysteine mutagenesis in conjunction with thiol-specific fluorescent labelling to characterize the interaction of Cyt2Aa1 with membranes, and potentially also the interaction of subunits within oligomers that may form on the membrane. To carry out this plan, one would need cysteine mutants that remain functionally active after labelling, so that one may assume their behaviour to reflect that of the wild-type toxin.

The mutants that were constructed as part of this work, however, turned out to be functionally inhibited or even entirely inactive. While they thus could not be used as models of the native toxin, their altered activity could nevertheless be analysed in order to gain insight in the mode of action of Cyt2Aa1. The results of these experiments support a model in which oligomers of heterogeneous subunit stoichiometry form discrete pores of heterogeneous functional diameter.

Chapter 2

Antibacterial activity of *B. thuringiensis* Cyt2Aa1 toxin

2.1 INTRODUCTION

While the δ-toxins of *B. thuringiensis* are most widely known for their effects against insect larvae, they are also active against other eukaryotic cells; red blood cells, in particular, are often used as membrane models for studying these toxins in vitro. Moreover, some δ-toxins also have antibacterial activity. This was first shown by Yudina and coworkers (see [72] and references cited therein). These researchers found that both CytA (Cyt1Aa1) and two different Cry toxins inhibited the growth of *Micrococcus luteus* and several other Gram-positive bacteria. The antibacterial effect required proteolytic activation of the toxins. A later study by Yudina and coworkers [73] observed antibacterial activity of Cry toxins also on clostridia and on the archaeal species *Methanosarcina barkeri*.

The antibacterial effect of Cyt toxin was addressed in studies by Itsko and coworkers [74, 75]. Cyt1Aa1 has high antibacterial activity, and the toxin even kills *E. coli* when recombinantly expressed in this host. In an earlier study [71], another *Bt* protein (P20) was characterized that, when co-expressed, protects *E. coli* from this lethal action.

In contrast to Cyt1Aa1, the Cyt family member Cyt1Ca is apparently inactive against bacteria, but introducing a few amino acid residues from Cyt1Aa1—namely, valine to replace aspartate in position 115, and alanine to replace asparagine in position 125—confers a degree of antibacterial activity [74]. A high level of antibacterial activity of externally applied Cyt1Aa1 against both Gram-positive and Gram-negative bacteria (*E. coli*) was reported by Cahan and coworkers [76].

In our studies [82] that involved the expression of Cyt2Aa1 in substantial amounts in *E. coli*, we did not observe an appreciable impact on bacterial viability, suggesting that Cyt2Aa1 may not have antibacterial activity. We decided to investigate the activity of Cyt2Aa1 against Gram-positive and Gram-negative model organisms.

2.2 MATERIALS AND METHODS

2.2.1 Plasmid construction, mutagenesis, and cloning

Plasmid pET-30a(+)Cyt2Aa1, which encodes the wild type toxin, was constructed by inserting a synthetic Cyt2Aa1 gene, codon-optimized for expression in *E. coli* (Integrated DNA Technologies; GenBank accession no. KM679365), into the expression vector pET-30a(+) (Novagen) between the BglII and XhoI cleavage sites located downstream of the T7 promoter.

The mutant V186C, which has previously been shown to retain full hemolytic activity after chemical modification [61] and was used here for thiol-specific derivatization with fluorescein maleimide, was constructed by PCR mutagenesis, using the synthetic primer pair 5'-GCAGTCATCGCGTGTCTGCCGCTGGCG-3' and 3'-CGCCAGCGGCAGACACGCGATGACTGC-5'. The plasmid DNA of Cyt2Aa1 in the pET-30a(+) vector was used as a template, and KOD (*Thermococcus kodakaraensis*) DNA polymerase (Novagen, Madison, WI) and the accompanying nucleotides and buffers were used as described by the manufacturer. The reaction mixture was incubated at an initial hold temperature of

95°C for 2 minutes, followed by 18 cycles of 95°C for 30 s, 55°C for 30 s, and 72°C for 60 s, followed by a final hold interval of 10 min at 74°C. PCR products were digested with the restriction enzyme Dpn1 (Fermentas) to destroy the template DNA before transformation.

The two plasmids containing the wild-type and the mutant cyt2Aa1 gene, respectively, were then transformed by electroporation into *E. coli* BL21(DE3) cells [83] for expression.

2.2.2 Expression and purification of Cyt2Aa1 toxin

A fresh single colony of *E. coli* BL21(DE3) containing cyt2Aa1 wild type gene or the V186C single cysteine mutant gene was grown at 37°C overnight in 15 mL of 2×YT medium (5 g/L NaCl, 16 g/L tryptone, 10 g/L yeast extract) containing 30 mg/L kanamycin. The overnight culture was then added to 1 liter of 2×YT medium containing 30 mg/L kanamycin. The culture was shaken vigorously (200 rpm) at 37°C until the OD_{600} reached 0.6. Expression of Cyt2Aa1 was induced by addition of 1mM isopropyl-β-D-thiogalactoside (IPTG), and the culture was then shaken slowly (150 rpm) overnight at 25°C.

The cells were harvested by centrifugation for 10 minutes at 4°C and 10,000×g. The cell pellet was resuspended in Tris 20 mM, NaCl 150 mM, pH 8.0 (TBS) and lysed using an emulsifier (Avestin Emulsiflex-C5) at 15,000 psi [84]. The cell lysate was centrifuged for 20 min at 20,000×g and 4°C. The pellet was resuspended by vortexing with 150 mL of ice-cold distilled water and then centrifuged again as before; this washing step was repeated three times. The pellet was then resuspended in 15 mL of phosphate-buffered saline (PBS; 8 mM Na_2HPO_4, 1.5 mM KH_2PO_4, 140 mM NaCl and 2.7 mM KCl, pH 7.4) and stored at −80°C. After thawing, the pellets were solubilized by incubation for 1 h at 37°C in 50 mM Na_2CO_3, pH 10.5. The solubilized toxin was separated from remaining insoluble material by centrifugation at 13,000×g for 20 min and stored at −20 °C. Despite the lack of a chromatographic purification step, the toxin produced by this procedure was pure as judged

by SDS-PAGE; this result agrees with previous reports [57]. The residual contaminant bands were further reduced during the subsequent proteolytic activation step (Figure 2.1A). Toxin concentrations were determined by absorption at 280 nm using a NanoDrop 2000 absorbance reader (Thermo Scientific, Wilmington, Del.).

The proteolytic activation of wild type and V186C mutant protoxin was performed with proteinase K, using conditions similar to those reported in [61] (1% w/w relative to protoxin, incubation at 37°C for 1h). After incubation, proteinase K was inactivated by addition of phenylmethylsulfonyl fluoride (PMSF) to 2 mM, and the activated toxin was transferred to PBS buffer (pH 7.4) using gel filtration on Sephadex G25. The toxin was sterile-filtered immediately before use in experiments with cells.

2.2.3 Hemolysis assay

Sheep red blood cells (RBCs, Cedarlane, Hornby, ON) were washed three times with PBS buffer by centrifugation. The washed RBCs were resuspended in PBS to a final concentration of 2% (v/v). 100 µL of the RBC suspension was added to the wells of a 96-well microtitre plate containing 100 µL of activated Cyt2Aa1 at the final concentrations indicated in the Results section. Hemolysis was detected by measuring the decrease in the optical density at 600 nm (OD_{600}), which is outside the absorption spectrum of hemoglobin and therefore simply represents cell turbidity. Unless stated otherwise, time-based measurements were performed at 25°C and were begun immediately after mixing the toxin with the red blood cells. All measurements were performed with a Spectramax 190 microplate reader (Molecular Devices, Sunnyvale, CA).

2.2.4 Labeling of Cyt2Aa1-V186C with fluorescein-5- maleimide

The proteolytically activated Cyt2Aa1-V186C mutant was mixed with 5 mM dithiothreitol (DTT) and incubated for 10 min at room temperature to reduce any disulfide bonds before labeling. The reduced protein

was transferred to PBS buffer (pH 7.4) before labeling using a PD10 (Sephadex G25) column in order to remove the DTT. Fluorescein-5-maleimide (Anaspec; 2 mM final concentration) was added to the protein, which was at 10 mg/mL (435 µM). The reaction mixture was incubated for 2 hours at room temperature. Dithiothreitol (DTT) was added to a final concentration of 2 mM to stop the labelling reaction. Excess dye was removed by gel filtration on Sephadex G25 equilibrated with PBS. The concentration of the labelled Cyt2Aa1-V186C was determined by using a NanoDrop absorbance reader (NanoDrop 2000, ThermoScientific, Wilmington, USA), using a molar extinction coefficient ε_{495} for fluorescein-5-maleimide of 68,000/M×cm (as stated by the supplier).

2.2.5 Growth inhibition in liquid culture

Liquid cultures of *Bacillus megaterium* ATCC-14581, *Bacillus thuringiensis* subsp. *kurstaki*, strain YBT-1520, and *Escherichia coli* DH5α, ATCC-67878 were grown in LB broth (10 g/L of tryptone, 5 g/L of yeast extract, and 10 g/L of NaCl). The two *Bacillus* strains were grown at 30°C, whereas *E. coli* was grown at 37°C. For growth curves, fresh liquid cultures were inoculated 1:1000 with an overnight culture, simultaneously with the addition of Cyt2Aa1 toxin and/or phenylmethylsulfonyl fluoride (PMSF, 2mM final concentration) as indicated. For each set of conditions, triplicate cultures were grown in separate wells of a microtitre plate. The microtitre plates were incubated without shaking at the temperatures indicated above, and the optical density was determined at hourly intervals.

2.2.6 Cell viability assay

A freshly isolated colony of the bacterial test strain in question was used to inoculate a fresh liquid culture in LB broth, which was grown with shaking (200 rpm) at 30°C (*B. megaterium* and *B. thuringiensis*) or 37°C (*E. coli*) for four hours. Cells were centrifuged for 5 minutes at

5000×g at 4°C. The cell pellets were resuspended in PBS and washed three times by centrifugation. The final suspension in PBS was adjusted to an OD_{600} of 0.6. The cells were then mixed with proteolytically activated Cyt2Aa1 toxin at various concentrations (1–10 mg/mL) and incubated for 1 hour at 37°C. Both toxin-treated and untreated control cells were stained using the Live/Dead BacLight bacterial viability kit (L7012, Molecular Probe, USA), which employs the two fluorescent dyes propidium iodide and SYTO9, according to manufacturer's instructions. The fluorescence was observed using a fluorescence microscope (Nikon Eclipse E600FN) and a digital camera (Nikon Digital Sight DS-U1).

2.2.7 Preparation of *Bacillus megaterium* protoplasts

A fresh colony of *B. megaterium* ATCC-14581 was used to inoculate a fresh 50 mL liquid culture in LB broth, which was grown with shaking at 30°C for four hours. Cells were centrifuged for 5 minutes at 5000×g at 4°C, then resuspended in PBS and washed three times by centrifugation. Cells were then suspended in PBS with 20% (w/v) sucrose and adjusted to an OD_{600} of 0.6. Lysozyme (Fluka) was added to a final concentration of 300 µg/mL and the cell suspension was incubated for 30 min at 37°C. Protoplasts were harvested by centrifugation for 5 minutes at 10,000×g at 4°C. The supernatant was discarded and the cell pellets were rapidly resuspended in PBS with 20% (w/v) sucrose. They were adjusted to an OD_{600} of 0.7 and used instantly for testing the lysis by Cyt2Aa1 toxin.

2.2.8 Lysis of *Bacillus megaterium* protoplasts by Cyt2Aa1 toxin

Freshly prepared *B. megaterium* protoplasts were incubated with activated Cyt2Aa1 toxin at a final concentration of 700 µg/mL at room temperature. Disintegration of protoplasts was monitored by the change in OD_{600} for two hours.

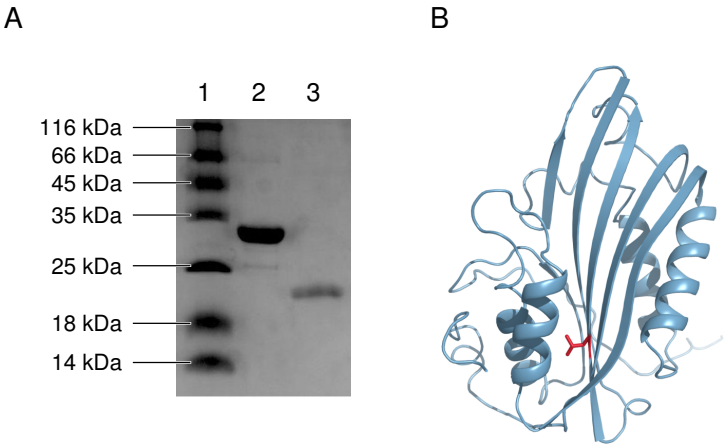

Figure 2.1 Preparation of activated Cyt2Aa1 toxin, and location of the V186C mutation. A: SDS-PAGE of Cyt2Aa1 protoxin (lane 2) and proteinase K-activated toxin (lane 3). Lane 1 shows a molecular weight standard. B: Location of the residue V186 (shown in red), which was replaced here with a mutant cysteine residue for the sake of thiol-specific modification with fluorescein maleimide. Structure rendered from 1cby.pdb. Binding of the fluorescein-labelled mutant to cell membranes is shown in Figure 2.5.

2.2.9 Calcein release experiments

Cells were grown, washed, and resuspended in PBS as described for the cell viability assay and then incubated with calcein acetoxymethyl ester (calcein AM, Sigma Aldrich) at a final concentration of 10 µg/mL for 1h at 37°C. The calcein-loaded cells were separated from excess calcein AM by centrifugation for 1 min at 5000×g at 4°C and then washed once more by centrifugation. They were resuspended in PBS and mixed with activated Cyt2Aa1 toxin at various concentrations as indicated in the Results section, incubated for 1 h at 37°C, and then observed by fluorescence microscopy as described above.

2.3 RESULTS AND DISCUSSION

2.3.1 Preparation of wild type and V186C mutant Cyt2Aa1 toxin

The two toxin species were successfully obtained using previously established methods [61]. Figure 2.1A illustrates an SDS-PAGE of the protoxin and the proteinase K-activated form. Figure 2.1B indicates the location of residue V186 [85], which was replaced with cysteine for the sake of thiol-specific fluorescent labeling. In keeping with reference [61], the hemolytic activity of the labelled mutant toxin was found to be undiminished relative to that of wild type toxin (data not shown).

2.3.2 Bacterial growth inhibition by Cyt2Aa1 toxin

The antibacterial activity of Cyt2Aa1 was assayed by adding the activated and sterile-filtered toxin to liquid cultures of the organism in question, at the time of inoculation. Growth curves were obtained by observing the change in the optical density at 600 nm.

Figure 2.2 shows typical growth curves for the *Bacillus megaterium* strain ATCC-14581 (A), *Bacillus thuringiensis* subsp. *kurstaki*, strain YBT-1520 (B), and *Escherichia coli* DH5α, ATCC-67878 (C). The growth of *B. megaterium* is readily suppressed by Cyt2Aa1 at 0.69 mg/mL, but gradually increases as the toxin is reduced toward 0.65 mg/mL; therefore, under these conditions, 0.69 mg/mL appears to be the minimum inhibitory concentration.

In order to examine the effect of the cell wall on the antibacterial activity of Cyt2Aa1, *B. megaterium* cells were converted to protoplasts with lysozyme and exposed to the toxin. As illustrated in Figure 2.3, the dosages of Cyt2Aa1 required to induce protoplast lysis were quite similar to those required for growth inhibition of regular vegetative cells, suggesting that the murein layer does not significantly augment or impede the antibacterial effect of the toxin.

With *B. thuringiensis*, the producer species of the toxin, growth is only weakly affected by Cyt2Aa1 even at 2 mg/mL (Figure 2.2B). *B. thu-*

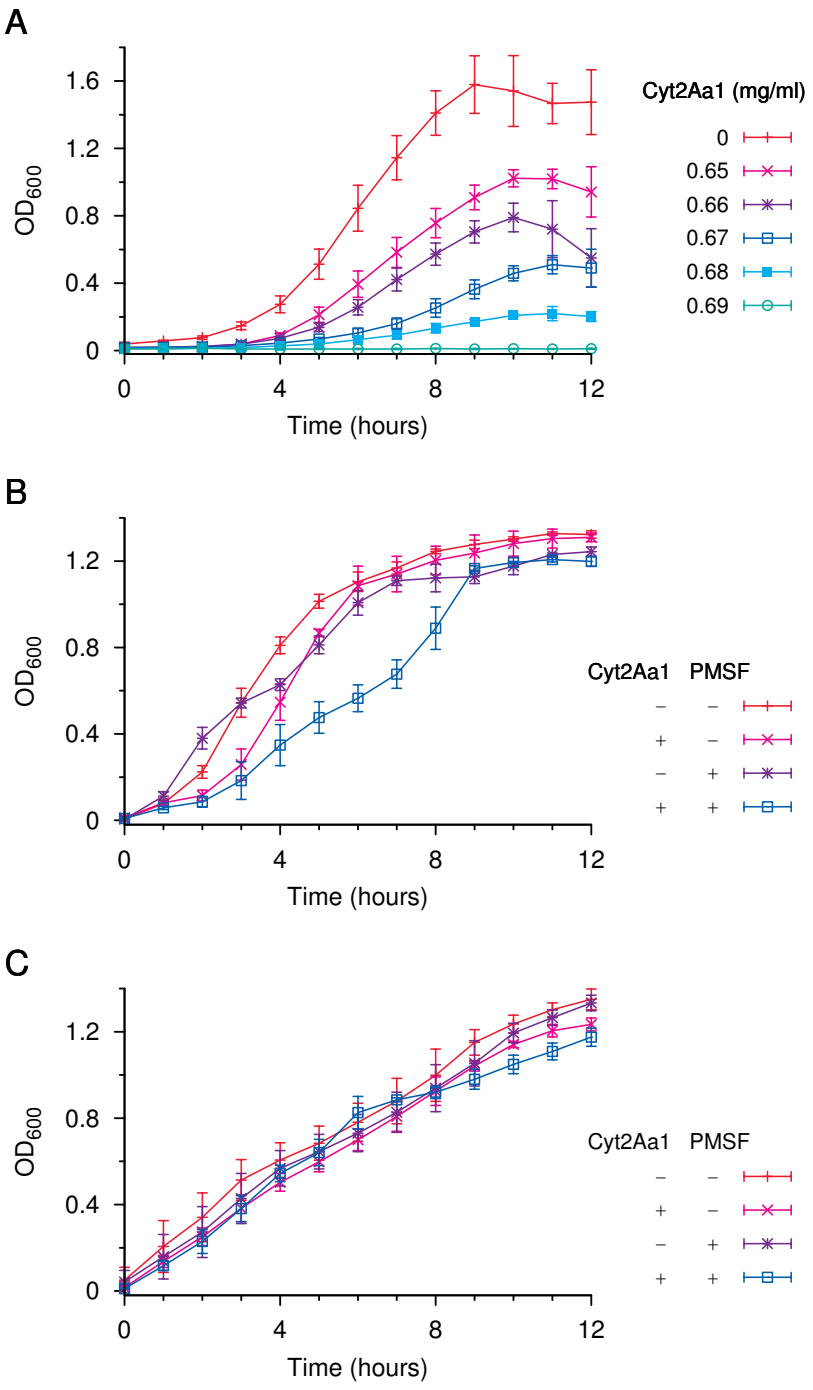

(Caption on following page)

ringiensis produces multiple exoproteases, including both serine and metalloenzymes [86], which might conceivably destroy the toxin before it can inhibit the growth of the bacterial cells. This is supported by the observation that bacterial growth is delayed by 2–3 hours when the same amount of Cyt2Aa1 is combined with the serine protease inhibitor phenylmethylsulfonyl fluoride (PMSF). The inhibitor alone had almost no effect on the growth rate. Considering that metalloenzymes would not respond to PMSF, and that PMSF in aqueous solution has a limited lifetime, the partial restoration of inhibitory activity by PMSF suggests that the cells are in principle susceptible to the toxin. This is also supported by the observation of calcein release from the cells (see below). With *E. coli*, the toxin at 2 mg/mL is virtually inactive, both with and without added PMSF (Figure 2.2C). Since *E. coli* DH5α is not known to produce exoproteases, the lack of an effect of PMSF is not surprising. Likewise, PMSF did not affect the activity of Cyt2Aa1 toxin on *Bacillus megaterium* (data not shown).

The bactericidal activity of Cyt2Aa1 was also examined using a commercially available fluorescence viability assay, which is based on the exclusion of the DNA-intercalating fluorescent dye um iodide by viable cells. The observations are illustrated in Figure 2.4 for *B. megaterium*. The green fluorescence in panel A is due to a second DNA-intercalating dye (SYTO 9) that enters both live and dead cells. Cells treated with

Figure 2.2 ***(preceding page)*** Inhibition of bacterial growth by Cyt2Aa1 toxin. Liquid cultures in LB medium were inoculated in triplicates at t=0 with 1:1000 volume of an overnight culture of the respective species. The toxin and PMSF were added at t=0. The OD_{600} was measured at hourly intervals. Controls contained cells in medium without toxin. Error bars represent standard deviations from three parallel experiments. A: *Bacillus megaterium* ATCC-14581. B: *Bacillus thuringiensis* subsp. kurstaki, strain YBT-1520. C: *E. coli* DH5α. In B and C, PMSF was used at a final concentration of 2 mM, and the toxin concentration was 2 mg/mL. None of the samples shown in A contained PMSF.

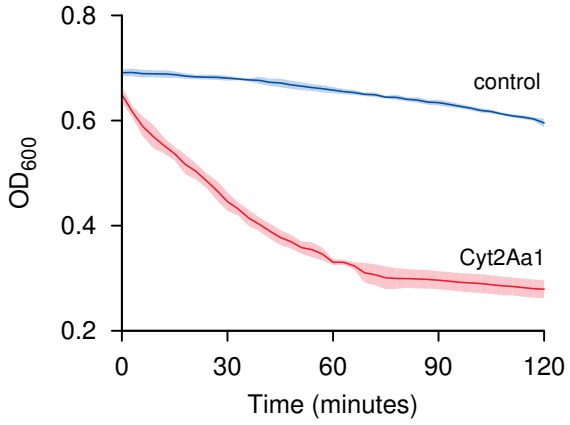

Figure 2.3 Lysis of *B. megaterium* protoplasts by Cyt2Aa1 toxin. Freshly prepared *B. megaterium* protoplasts were adjusted to an OD of 0.7 and then treated with activated wild type Cyt2Aa1 at a final concentration of 700 µg/mL. The control sample contained *B. megaterium* protoplasts incubated without Cyt2Aa1. The bands around each curve represent $\pm$ standard deviation from three separate concurrent experiments.

Cyt2Aa1 exhibit red fluorescence, which indicates that propidium has entered and also bound to DNA, resulting in the quenching of SYTO9 fluorescence. This is characteristic of dead bacterial cells [87].

2.3.3 Antibacterial mode of action of Cyt2Aa1

The Cyt toxins damage insect cells by binding and permeabilizing cell membranes. We examined whether the same action mode also applies to susceptible bacteria. To detect binding, we used a single cysteine mutant (V186C), which, as has been shown previously, can be labelled on the mutant cysteine residue without losing cytolytic activity [61]. The mutant was thiol-specifically derivatized with fluorescein maleimide and incubated with *B. megaterium* (Figure 2.5A) or *B. thuringiensis* (Figure 2.5B), and the cells were then examined by fluorescence microscopy. The cells were visibly stained, which confirms binding of the toxin to the bacterial cells. Since there is no known mechanism for

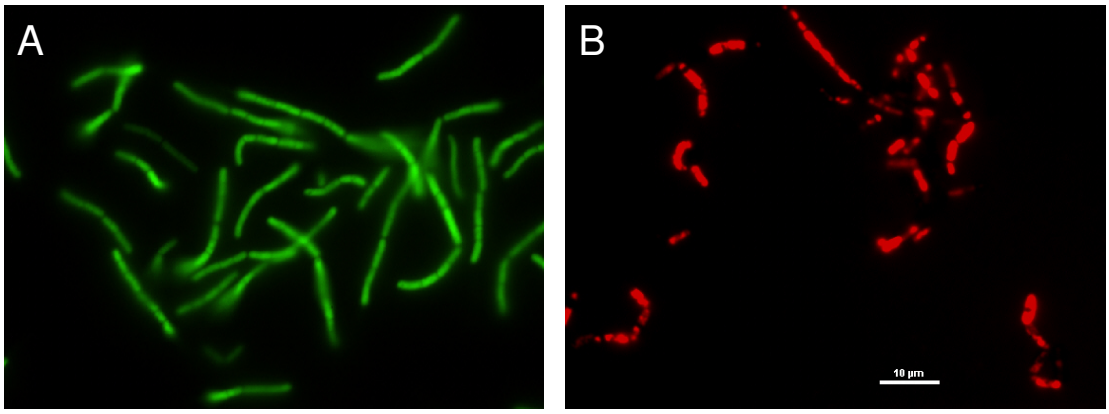

Figure 2.4 Effect of Cyt2Aa1 on *Bacillus megaterium* using the BacLight viability assay. *B. megaterium* ATCC-14581 cells were incubated with SYTO9 and propidium iodide, without prior treatment with 10 mg/mL Cyt2Aa1 toxin for 60 minutes. A: Control without toxin treatment. The intense green fluorescence is characteristic of viable cells that admit SYTO9 but exclude propidium iodide. B: Toxin-treated cells. Red fluorescence indicates penetration of propidium iodide into non-viable cells.

translocation of Cyt toxins across the membrane into the cytoplasm, it seems likely that the labelled toxin is bound to the cell membrane. No binding was observed with *E. coli* DH5α (Figure 2.5C), which agrees with the absence of toxin activity against this species.[1]

In *B. megaterium* and *B. thuringiensis*, membrane permeabilization by Cyt2Aa1 was confirmed with a calcein release assay. Calcein is a negatively charged, membrane-impermeant fluorescein derivative that can be loaded into living cells as its neutral and more hydrophobic acetoxymethyl ester. Inside the cell, the ester undergoes hydrolysis, causing the free dye to remain trapped within the cell. Both *B. megaterium* (Figure 2.6A) and *B. thuringiensis* (Figure 2.6C) could be stained in this manner. After incubation with Cyt2Aa1 (Figure 2.6B and D, respec-

[1]Figure 2.5D shows the binding of the labelled Cyt2Aa1 toxin to red blood cells, which are intended as a positive control. In this sample, several cells appear non-fluorescent. These may have failed to be lysed by the toxin, and the retained hemoglobin may have quenched the fluorescence of the bound toxin.

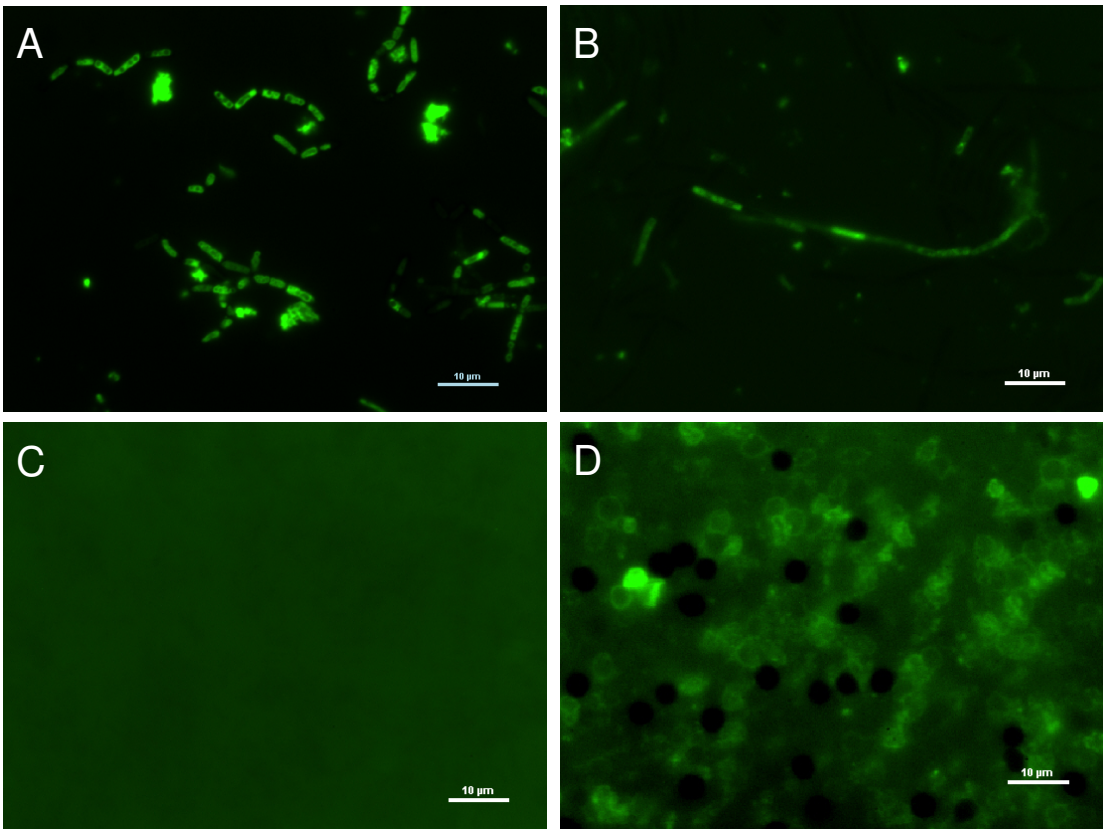

Figure 2.5 Binding of fluorescein-labelled Cyt2Aa1 toxin to bacterial cells and red blood cell ghosts. Cells of *Bacillus megaterium* (A), *Bacillus thuringiensis* (B), *Escherichia coli* DH5α, as well as sheep red blood cells (D) were incubated for 60 minutes with fluorescein-labelled Cyt2Aa1 mutant V186C at 10 mg/mL final concentration, washed by centrifugation, and examined by fluorescence microscopy. The toxin binds to the two *Bacillus* species but not to *E. coli*. It also binds to most of the red blood cell membranes.

tively), most of the calcein is released from the cells, indicating that the membranes have become permeabilized. This supports the notion that the toxin permeabilizes bacterial cells, and therefore acts on bacterial cell membranes in the same manner as on insect cells.

Overall, the findings of our studies support the previous conclusion that Cyt toxins do have antibacterial activity. However, the antibacterial

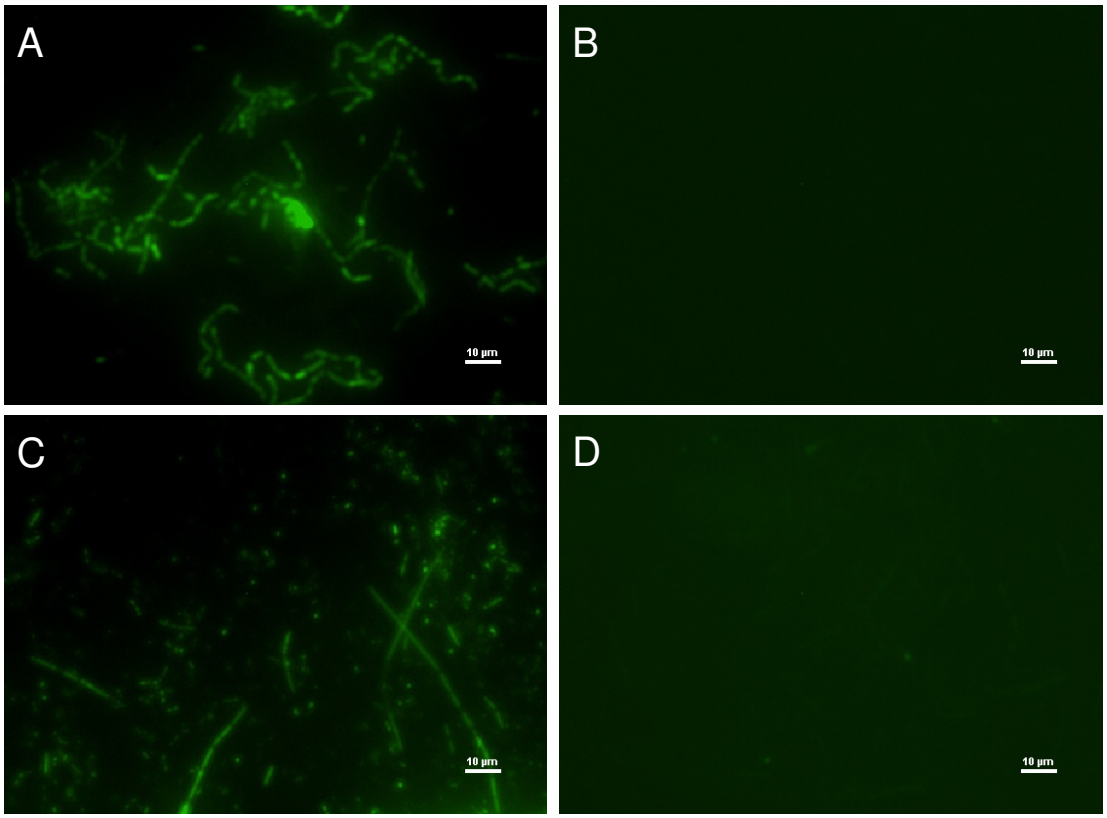

Figure 2.6 Release of calcein by Cyt2Aa1 toxin from bacterial cells. Cells of *Bacillus megaterium* (A,B) or *Bacillus thuringiensis* (C,D) were loaded with calcein acetoxymethyl ester and then incubated without (A,C) or with (B,D) Cyt2Aa1 toxin at 5 mg/mL for 60 minutes. Green fluorescence indicates retention of the dye within the bacterial cells.

activity of Cyt2Aa1 is several orders of magnitude lower than that of Cyt1Aa1 [72, 76], and it has no detectable activity against *E. coli*. This agrees with our observation that Cyt2Aa1 can be expressed at high levels in *E. coli* cells, which is not possible with Cyt1Aa1 in the absence of accessory proteins from *B. thuringiensis* that inhibit the antibacterial effect [71].

Absence of activity against *E. coli* has previously been reported for another Cyt toxin, Cyt1Ca; replacement of several amino acids so as

to convert them to the homologous residues in Cyt1Aa1 introduced a low degree of antibacterial activity [74]. Thus, there is precedent of substantial differences in antibacterial activity between different members of the Cyt toxin family. Creation of Cyt1Aa1/Cyt2Aa1 chimeras might be worthwhile to identify the molecular determinants of the large difference in antibacterial activity.

Our findings also suggest that the action mode on bacterial cells is analogous to that on insect cells and red blood cells, and that it is mediated by the formation of transmembrane pores. The toxin binds to the cell surface in an apparently uniform manner, without causing their outright disruption, as would be expected with an antimicrobial peptide-like mechanism (Section 1.2). The toxin releases calcein from the cells, and toxin-exposed cells fail to exclude propidium iodide, which by analogy to ethidium bromide [88] is most likely a substrate for membrane potential-dependent efflux pumps. All these observations point to the formation of discrete membrane lesions, that is, transmembrane pores, as the key mechanism of antimicrobial activity.

Chapter 3

The role of cholesterol in the activity of Cyt2Aa1 toxin

3.1 INTRODUCTION

In Chapter 2, we examined the activity of Cyt2Aa1 toxin on bacterial cells. While the toxin was found to be active on Gram-positive bacteria, its specific activity on the bacterial cell membranes is orders of magnitude lower than that reported for insect cells and for red blood cells or other mammalian cells [57, 68]. Since no specific receptor for the Cyt toxins is known, the pronounced differences in susceptibility are currently unexplained.

A key difference between the membranes of animal cells—both insect and mammalian—and those of bacterial cells is the presence of cholesterol in the former but not the latter. With several families of pore-forming bacterial toxins, membrane cholesterol is required for activity, which provides a straightforward strategy for the bacteria in question to protect themselves from their own toxins and to target them exclusively to animal membranes. Examples of such cholesterol-dependent pore-formers include streptolysin O and its homologues from Gram-positive

bacteria, which are collectively referred to as the "cholesterol-dependent cytolysins," as well as the structurally unrelated *Vibrio cholerae* cytolysin [32]. Since Cyt2Aa1 resembles these toxins in showing much greater activity on animal cells than on bacterial cells, the possibility arises that cholesterol facilitates the activity of this toxin also.

Another relevant observation is the difference in cholesterol content between mammalian and insect cell membranes. Insects are auxotrophic for cholesterol [89], and the concentration of the sterol relative to phospholipids is roughly half as high as that typical of mammalian cells [90]. Since insect cells and mammalian cells are similarly susceptible to Cyt2Aa1, one might therefore expect that any effects of cholesterol take hold already at fairly low concentrations in the membrane.

In light of these considerations, it appeared pertinent to examine the effect of cholesterol on the activity of Cyt2Aa1 toxin. In this chapter, the effect of cholesterol was investigated using sheep red blood cells and liposomes as model systems.

3.2 MATERIALS AND METHODS

3.2.1 Expression and purification of Cyt2Aa1; hemolytic activity assay

These were performed as described before in Section 2.2.2.

3.2.2 Cholesterol extraction with methyl-β-cyclodextrin

Methyl-β-cyclodextrin (Sigma Aldrich, St. Lous, MO) was dissolved to 10 mM in PBS (8 mM Na_2HPO_4,1.5 mM KH_2PO_4, 140 mM NaCl, and 2.7 mM KCl; pH 7.4) and then sterilized by filtering through an Acrodisk 0.25 µm filter (Pall Corporation, MI). Sheep RBCs (1 ml, 50% v/v) were washed three times with PBS and incubated in 1 mL of PBS containing the desired final concentrations of methyl-β-cyclodextrin for 2 hours at 37°C. The cells were then washed again twice with PBS and diluted as required. All hemolysis experiments involving methyl-β-cyclodextrin were done with freshly prepared cholesterol-depleted RBCs.

3.2.3 Cholesterol assay

To assess the extent of cholesterol depletion from red blood cells, 1 mL of the methyl-β-cyclodextrin (1-10 mM) treated RBCs as well as control cells not treated with methyl-β-cyclodextrin were lysed osmotically with a 5 mM potassium phosphate buffer, pH 7.4. The membranes were washed with the buffer several times by centrifugation until the hemoglobin pigment had completely disappeared. The cholesterol concentrations of the membranes were measured using a fluorescence-based coupled enzymatic assay (using Amplex® Red Cholesterol Assay, Invitrogen Molecular Probes, CA) according to the manufacturer's protocol. The assay solution contains cholesterol esterase in addition to cholesterol oxidase, and it therefore detects both free cholesterol and cholesteryl esters. All fluorescence readings were taken using a 96-well fluorescence microplate reader (Spectramax 190, Molecular Devices, Sunnyvale, CA).

3.2.4 Liposome preparation

Cholesterol, 1,2 dimyristoyl-sn-glycero-3-phosphocholine (DMPC) and 1,2-dimyristoyl-sn-glycero-3-phosphoglycerol (DMPG) were purchased from Avanti Polar Lipids (Alabaster, AL). The lipids were dissolved in chloroform and mixed in various molar ratios. The cholesterol content was varied as indicated in the Results section; DMPG accounted for 5 or 10% of the total, and DMPC made up the balance. The lipid solutions were dried down under a stream of nitrogen in a round-bottom flask for 5 minutes and then dried under vacuum for an additional 4 hours to remove any residual traces of chloroform. The dried lipids were resuspended by vortexing for 10 min with 1.5 mL of Hepes-buffered saline (HBS; 10 mM Hepes, 150 mM NaCl, pH 7.4) containing 50 mM calcein (Sigma Aldrich) at room temperature to a final total lipid concentration of 10 mg/mL. The resulting suspensions of multilamellar liposomes were sized down to unilamellar liposomes using a liposome extruder

(Northern Lipids, Vancouver, BC) by extruding 10 times through a 100-nm polycarbonate membrane filter (Whatman). Subsequently, non-encapsulated calcein was removed by chromatography using a Sepharose 6B (Sigma) column pre-equilibrated with HBS.

3.2.5 Calcein release assay

The calcein entrapped liposomes were diluted to 37.5 µg/mL (estimated) with HBS, mixed with activated Cyt2Aa1 toxin (final concentrations as indicated in the Results section), and then incubated for 1 hour at 37°C. The calcein fluorescence intensity was then measured (excitation, 470 nm; emission, 512 nm) on a QuantaMaster 4 spectrofluorimeter (PTI, London, ON). The extent of membrane permeabilization P was then calculated using the following formula:

$$P = \frac{F_{\text{sample}} - F_0}{F_{\text{Triton}} - F_0} \tag{3.1}$$

where F_0 is the fluorescence of a liposome control without toxin, and F_{Triton} is that of a liposome sample solubilized with Triton X-100 at a final concentration of 0.1%.

3.3 RESULTS

3.3.1 Hemolytic activity of Cyt2Aa1 toxin on native sheep erythrocytes

While hemolysis is often measured by the absorption of the released hemoglobin, an even more straightforward methods uses the turbidity caused by the remaining intact cells, which can be monitored in real time. This can be accomplished by observing the optical density at 600 nm, which is outside the absorption spectrum of hemoglobin.

As can be seen in Figure 3.1, hemolysis sets in more rapidly with increasing toxin concentrations; the acceleration is most pronounced

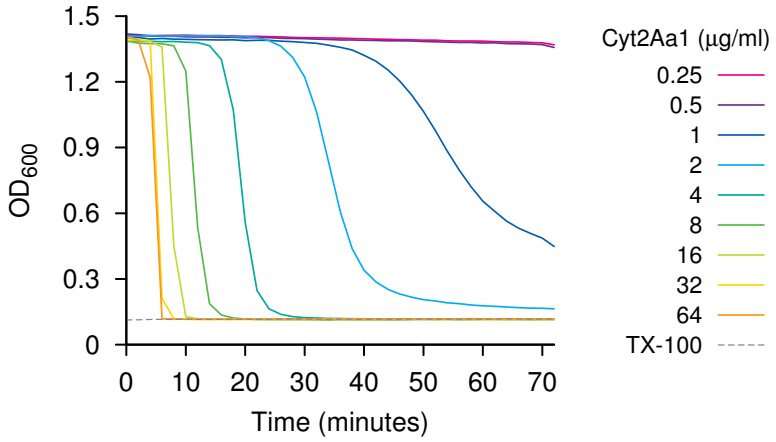

Figure 3.1 Hemolytic titration of Cyt2Aa1 toxin. Sheep red blood cells at 1% were supplemented at t=0 with the indicated concentrations of Cyt2Aa1 toxin. The OD_{600} at a given incubation time represents the fraction of cells remaining intact; a more rapid decline in OD indicates more rapid hemolysis.

with low concentrations and decreases at higher concentrations. Essentially complete hemolysis is achieved within one hour at toxin concentrations $\geq 2\,\mu g/mL$. This level of hemolytic activity is very similar to that of a previously characterized preparation of the same toxin [57]. Moreover, it is more than two orders of magnitude higher than the antibacterial activity characterized in the preceding chapter of this thesis, which confirms the premise of this study.

3.3.2 Cholesterol depletion of sheep red blood cells

Cholesterol can be extracted from cell membranes using β-cyclodextrin [91] and derivatives such as methyl- or hydroxypropyl-β-cyclodextrin [92]. The extent of cholesterol extraction from sheep red blood cells using different concentrations of methyl-β-cyclodextrin is depicted in Figure 3.2. An approximately linear relationship is apparent between the extent of depletion and the cyclodextrin concentration. While the graph represents the level of extraction achieved after two hours of in-

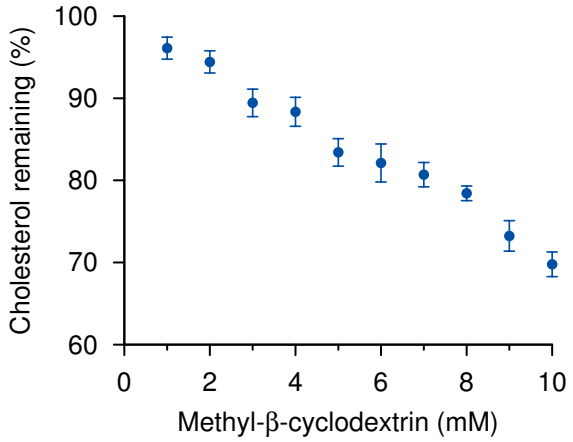

Figure 3.2 Cholesterol depletion of erythrocytes with methyl-β-cyclodextrin. The cells were incubated for 2 hours at 37℃ with methyl-β-cyclodextrin at the indicated concentrations. The cells were lysed osmotically, and the membranes washed by centrifugation. The amount of cholesterol remaining in the membranes was determined using a fluorescence-based coupled enzymatic assay. Error bars represent ± standard deviation of four independent experiments.

cubation, very similar data were observed after one hour (not shown), indicating that the extraction has reached or approached equilibrium. While the attainment of equilibrium after such periods of time is consistent with earlier studies on the kinetics of cholesterol transfer to methyl-β-cyclodextrin [92], the maximum extent of depletion is decidedly lower than reported previously with human erythrocytes [93] as well as other cell types [94].

In the experiments shown, the cells began to become hemolytic at methyl-β-cyclodextrin concentrations beyond 10 mM, indicating general membrane destabilization, which may be related to the extraction of not only cholesterol but also other membrane lipids [92]. In all experiments reported below, we therefore used no more than 10 mM of methyl-β-cyclodextrin.

3.3.3 Hemolytic activity of Cyt2Aa1 on cholesterol-depleted sheep erythrocytes

The activity of Cyt2Aa1 on red blood cells that had been partially depleted of cholesterol to different degrees using methyl-β-cyclodextrin was compared using the same assay as illustrated in Figure 3.1. The results are shown in Figure 3.3A. It can be seen that the time course of hemolysis is accelerated after exposure to low or intermediate concentrations of methyl-β-cyclodextrin. However, hemolysis slows again after exposure of the cells to methyl-β-cyclodextrin concentrations greater than 6 mM.

The effect is clearly observed only at Cyt2Aa1 concentrations up to 1.25 µg/mL, whereas at higher toxin concentrations, any effect of cholesterol depletion is hard to detect (Figure 3.3B and C). Overall, the effect is small, considering that the maximal hemolytic activity observed with 1 µg/mL, which occurs after cell treatment wit 3–6 mM methyl-β-cyclodextrin, is approximately equal to the activity of 1.25 µg/mL on native red blood cells. This may not be surprising in light of the fact that the extent of cholesterol depletion under these conditions is limited to 10–20% (cf. Figure 3.2).

3.3.4 Effect of membrane cholesterol content on liposome permeabilization by Cyt2Aa1

Cyclodextrin-mediated cholesterol extraction from natural membranes is incomplete and not entirely specific. A simpler and more readily controlled model system is provided by liposomes, which can be produced from almost arbitrary mixtures of lipids. Permeabilization of liposomes by pore-forming proteins and peptides can be monitored using entrapped fluorescent markers. One popular assay uses the release of calcein, a derivative of fluorescein. Like carboxyfluorescein [95], the fluorescence of calcein is subject to concentration-dependent self-quenching. When released by permeabilizing agents from the confined space

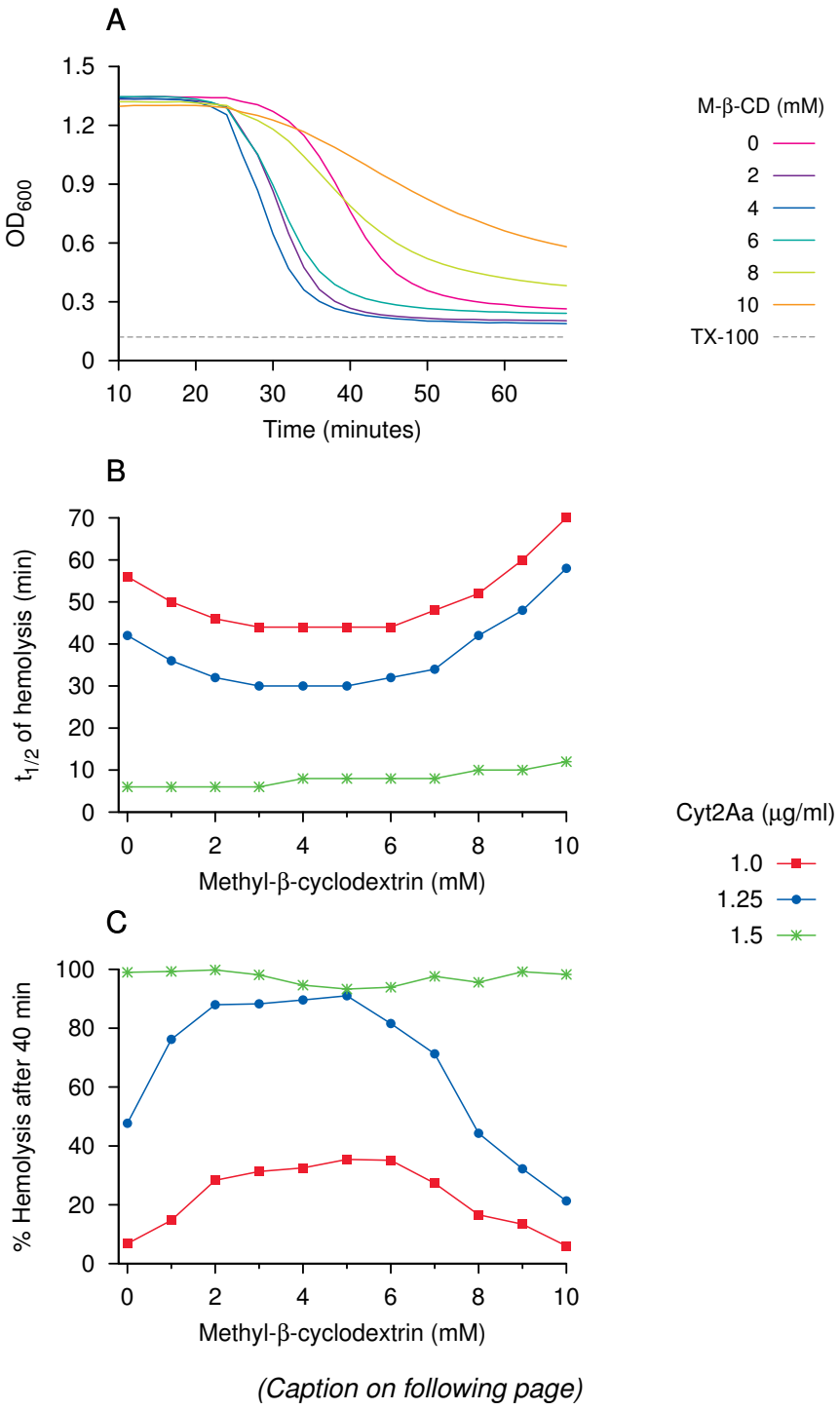

(Caption on following page)

inside the liposomes into the larger buffer volume, calcein is diluted, and its fluorescence increases.

In the experiments shown in Figure 3.4, it is seen that liposomes containing ≥20% cholesterol are almost impervious to Cyt2Aa1, whereas liposomes with no more than 10% cholesterol are quite susceptible; permeabilization reaches a half-maximal level at 10–20 µg/mL of Cyt2Aa1 with liposomes containing 0 or 10% cholesterol, which is about ten times higher than the toxin concentration required for hemolysis (cf. Figure 3.1). In contrast, liposomes with ≥20% cholesterol are virtually unaffected even at 400 µg/mL of Cyt2Aa1 (see Figure 3.4B and C). Thus, the effect of the sterol appears to be much stronger than that observed with red blood cells.

A curious intermediate behaviour is observed at 15% cholesterol. Liposomes with this composition are quite readily permeabilized at 60–80 µg/mL of Cyt2Aa1, but surprisingly show a lower degree of permeabilization at Cyt2Aa1 concentrations above 80 µg/mL. While unusual, such "prozone" phenomena have been reported with mutants of *Staphylococcus aureus* α-toxin [96] and with the serum complement system, [97], which are also proteins with pore-forming activity.

Figure 3.3 ***(preceding page)*** Effect of cholesterol depletion on the hemolytic activity of Cyt2Aa1. Sheep red blood cells, partially depleted of cholesterol with different concentrations of methyl-β-cyclodextrin as shown in Figure 3.2, were incubated with Cyt2Aa1. Hemolytic activity was measured as the decrease in OD_{600} as shown in Figure 3.1. A: Time course of hemolysis with 1.25 µg/mL of Cyt2Aa1. Activity increases up to 4 mM of methyl-β-cyclodextrin and then decreases again. B: Time required for 50% of hemolysis, as a function of methyl-β-cyclodextrin concentration, for three different concentrations of Cyt2Aa1. C: Extent of hemolysis after 40 minutes under the same conditions as in panel B.

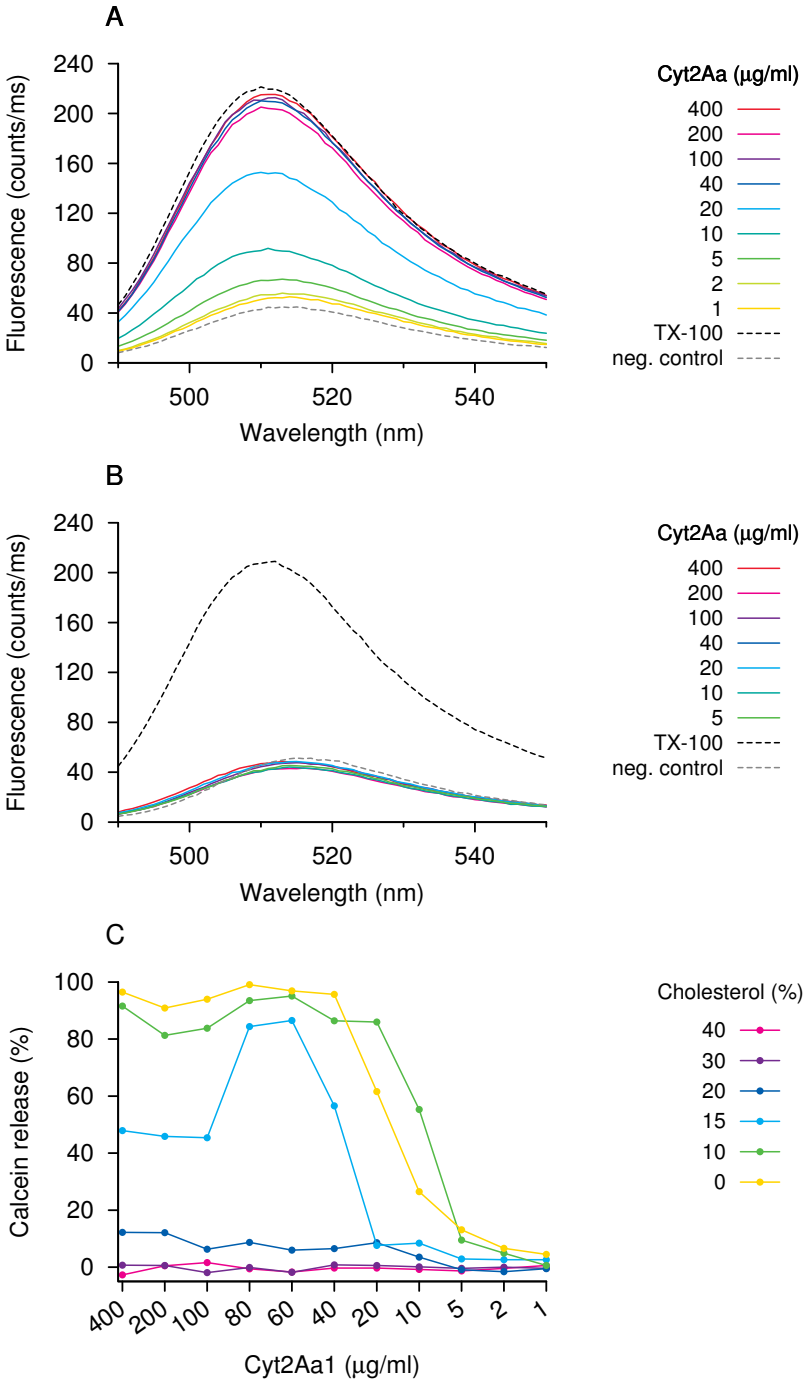

(Caption on following page)

3.4 DISCUSSION

As discussed in Section 3.1, previous findings on the susceptibility to Cyt2Aa1 toxin of bacterial, insect, and mammalian cell membranes gave reason to expect a role of cholesterol in the activity of the toxin. Intriguingly, as discussed in the introduction of this chapter, some of the evidence suggested that the sterol might support the activity, whereas other observations favoured an inhibitory effect.

The outcome of the experiments conducted here is somewhat divergent. With liposomes, which provide a simple and clean, yet artificial model system, cholesterol strongly inhibits Cyt2Aa1; as the mole fraction of cholesterol is reduced to below 20%, the activity of Cyt2Aa1 increases greatly. In contrast, with sheep red blood cells, the partial extraction of the sterol resulted in only minor effects on Cyt2Aa1 activity.

When comparing these two results, we need to consider that our procedure for cholesterol extraction removed only up to 30% of the sterol contained in the cells; all observed functional effects therefore occurred within a small range of residual cholesterol concentration. The observed extent of cholesterol depletion is relatively low when compared to previous studies that applied similar conditions to different cell types

Figure 3.4 ***(preceding page)*** Effect of cholesterol on the permeabilization of liposomes by Cyt2Aa1. Liposomes containing variable amounts of cholesterol were loaded with calcein and exposed to the toxin. Permeabilization causes an increase in calcein fluorescence. A: Liposomes without cholesterol are permeabilized by Cyt2Aa1. 100% calcein release is defined by solubilization with Triton-X100 (TX-100). B: Liposomes containing 40% of cholesterol are not permeabilized. C: Calcein release as a function of cholesterol. A steep transition from Cyt2Aa1 susceptibility to resistance occurs between 10 and 20% cholesterol. Liposomes containing 15% cholesterol display a “prozone phenomenon”, that is, they are less susceptible to very high than to intermediate Cyt2Aa1 concentrations.

[92, 94]. A possible explanation for this low degree of extraction relates to the composition of the other membrane lipids. The red blood cells of sheep and of other ruminants are exceptionally high in sphingomyelin, which replaces phosphatidylcholine (PC) as the dominant phospholipid in the cell membrane [98]. Like other sphingolipids, sphingomyelin has a higher affinity for cholesterol than does PC [99], a circumstance that is considered important in the formation and stabilization of lipid rafts [100].

Lowering the cholesterol level in red blood cell membranes did not only produce less of an increase in susceptibility to Cyt2Aa1 than in liposomes, but the trend even reversed altogether at methyl-β-cyclodextrin concentrations of ≥6 mM, an effect for which there is no parallel in the liposome experiments. It is not possible, however, to ascribe this observation with certainty to the variation in cholesterol concentration alone. One has to keep in mind that the affinity of cyclodextrins is not totally specific for individual lipid species. While β-cyclodextrin preferentially extracts cholesterol and α-cyclodextrin phospholipids, these preferences are not absolute, and at higher concentrations, β-cyclodextrin will begin to extract phospholipids also [91, 92, 101]. Such non-selective lipid extraction might explain why at methyl-β-cyclodextrin concentrations above 10 mM the red blood cells became unstable and underwent hemolysis even in the absence of any added Cyt2Aa1. Therefore, we conclude that the results of this chapter prove only an inhibitory effect of cholesterol, whereas the activating effect suggested by exposure of red blood cells to high concentrations of methyl-β-cyclodextrin remains uncertain.

The observed inhibition of Cyt2Aa1 activity by cholesterol obviously does not offer any explanation for the low susceptibility of Gram-positive bacteria described in Chapter 2. Moreover, it also is not reflected in any major difference in susceptibility to Cyt2Aa1 between insect and mammalian cells. In contrast to mammalian cells, which synthesize their own cholesterol as needed, insects are cholesterol aux-

otrophs [89], and insect cells thus contain only approximately half as much cholesterol than mammalian cells [90, 102, 103]. On both insect cells and mammalian cells, the activity of Cyt2Aa1 exceeds that on even the most susceptible ones of the model liposomes examined here. This shows that Cyt2Aa1 activity is more strongly influenced by specific membrane constituents other than cholesterol. While nothing is known yet about any such sensitizing membrane lipids or proteins, our results indicate that they exist, and hence future research should be directed at their characterization.

A curious phenomenon was observed with liposomes that contained 15% cholesterol: the extent of permeabilization by Cyt2Aa1 was lower with high concentrations of the toxin than with intermediate ones (Figure 3.4). Such so-called "prozone" effects are fairly common in laboratory tests that use serum complement, such as the complement fixation test. While the complement system produces an oligomeric transmembrane pore [104], the mechanism of prozone effects is not closely related to the pore formation itself, but rather to the preceding step of antibody-mediated complement activation: antibody isotypes that fail to activate complement may compete with activating ones for the antigen [97, 105].

There is, however, another precedent that may be more apposite. The study in question concerns *Staphylococcus aureus* α-hemolysin (cf. Section 1.2.1), several point mutants of which exhibited a similar prozone effect in a hemolytic titration assay [96]. While α-hemolysin normally forms highly regular, heptameric pores [106], the oligomers formed by those same mutants also exhibited irregularities and imperfections as judged by electron microscopy.

While there is thus precedent of prozone phenomena with pore-forming toxins, it seems difficult to reconcile this observation with the proposed detergent-like mechanism that has been proposed for the Cyt toxins [59, 69]; the literature does not provide examples of any antimicrobial peptides or similar molecules that inhibit such an effect. Therefore, our observation appears to favour the formation of discrete,

oligomeric pores as the action mechanism of Cyt2Aa1 and likely of other Cyt toxins.

Chapter 4

Studies on the mechanism of membrane permeabilization by Cyt2Aa1

4.1 INTRODUCTION

With many pore-forming toxins, a successful strategy for correlating structure and function has been the use of cysteine mutagenesis in combination with thiol-specific labelling with environmentally sensitive fluorescent dyes (for examples, see [107–109]). This approach is most useful if the mutants are readily amenable to covalent modification and remain functionally active after labelling, since spectral changes observed with such active derivatives can be correlated with the behaviour of the wild-type protein.

In the work that is described in this chapter, we attempted to apply this strategy to Cyt2Aa1. A series of cysteine mutants—S166C, S194C, S210C, and Q224C—was generated, but as shown below, none of these were fully functional. They were therefore not considered suitable models for the wild-type toxin, and we did not perform extensive

Table 4.1 Primers used for site-directed PCR mutagenesis

Mutant	Orientation	Sequence (5'→3')
S166C	forward	GCCCACAACACCTGCTACTACTACAACATTCTGTTCAGC
	reverse	GCTGAACAGAATGTTGTAGTAGTAGCAGGTGTTGTGGGC
S194C	forward	CGCGGTTCTGCCGCTGGCGTTTGAAGTGTGCGTCG
	reverse	CGACGCACACTTCAAACGCCAGCGGCAGAACCGCG
S210C	forward	CCATCAAGGACTGCGCTCGCTACGAGG
	reverse	CCTCGTAGCGAGCGCAGTCCTTGATGG
Q224C	forward	GCTCACCCTGGTCTGCGCTCTGCACTCTTCTAACGCG
	reverse	CGCGTTAGAAGAGTGCAGAGCGCAGACCAGGGTGAGC

fluorescence studies on them. Instead, we examined their functionally deficient phenotypes and their interaction with wild-type Cyt2Aa1, which produced some interesting insight into the action mode of the toxin.

4.2 MATERIALS AND METHODS

Methods for protein expression, purification, and proteolytic activation of Cyt2Aa1 and its mutant derivatives have been described in Section 2.2, and those for hemolytic assays and liposome preparation can be found in Section 3.2.

4.2.1 Site-directed mutagenesis

The experimental protocol used has been described in Section 2.2.1. Primer pairs for the mutants generated here are listed in Table 4.1.

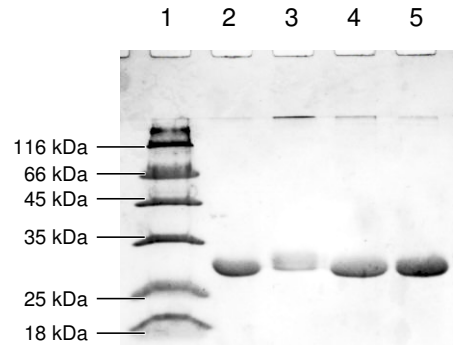

Figure 4.1 SDS-PAGE of single cysteine mutants after proteinase K activation. Lane 1: molecular weight standard; 2: S166C; 3: S194C; 4: S210C; 5: Q224C.

4.2.2 Hemolysis experiments

Preparation of the red blood cell suspension and monitoring of OD_{600} were carried out as described in Section 2.2.3. In some of the experiments describe here, the assay was modified by adding a preincubation stage at 4°C, during which wild-type and mutant toxins were sequentially added. The samples were then transferred to room temperature to start the hemolysis reaction.

In a second series of experiments, the red blood cell suspension was prepared in PBS containing PEG 1000 at 20% (v/v); the final concentration of PEG in the hemolysis reaction was 10% (v/v).

4.3 RESULTS

4.3.1 Construction and expression of cysteine mutants

The mutants were generated, expressed, and activated with proteinase K as described in Section 2.2. After limited proteolysis, all mutants showed a molecular weight similar to that of wild-type toxin (see Figure 4.1). Proteinase K has broad amino acid specificity, and therefore cleavage is likely limited by conformational rather than by chemical

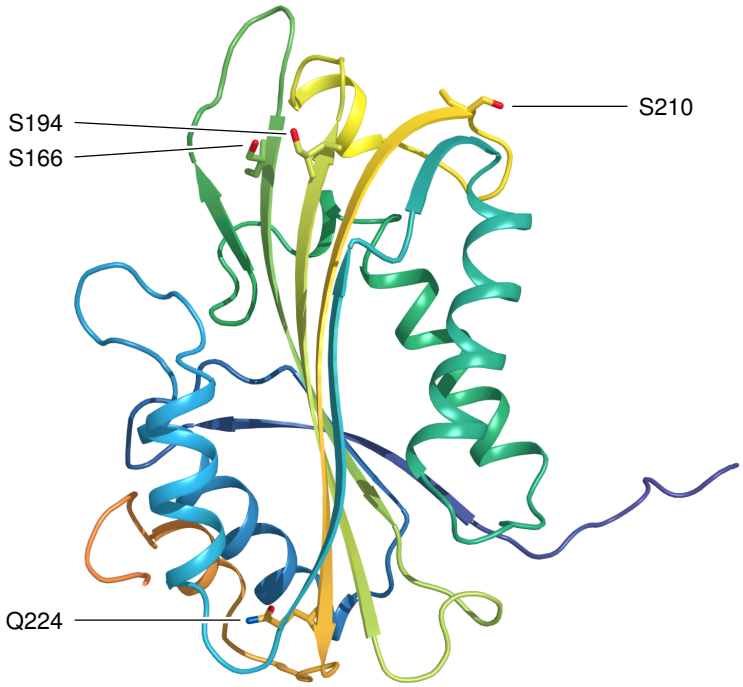

Figure 4.2 Positions of the mutant residues S166C, S194C, S210C and Q224C in the Cyt2Aa1 monomer. The N-terminus of the polypeptide chain is shown in blue, and the C-terminus in orange. The side chains of the mutated residues are shown in stick representation. The side chains of all mutant residues are at the surface of the molecule.

constraints. Therefore, the similarity of the products generated by limited proteinase K treatment suggests that the mutants are correctly folded.

Figure 4.2 shows the positions of the mutant residues. All residues are located at or close to the molecular surface, which should facilitate covalent derivatization of the natively folded mutant molecules. In addition, three of the mutant residues are serines. Since serine differs from cysteine by only one atom, it was expected that at least the unlabelled mutants should retain hemolytic activity. As shown in the next section, however, this expectation proved to be wrong.

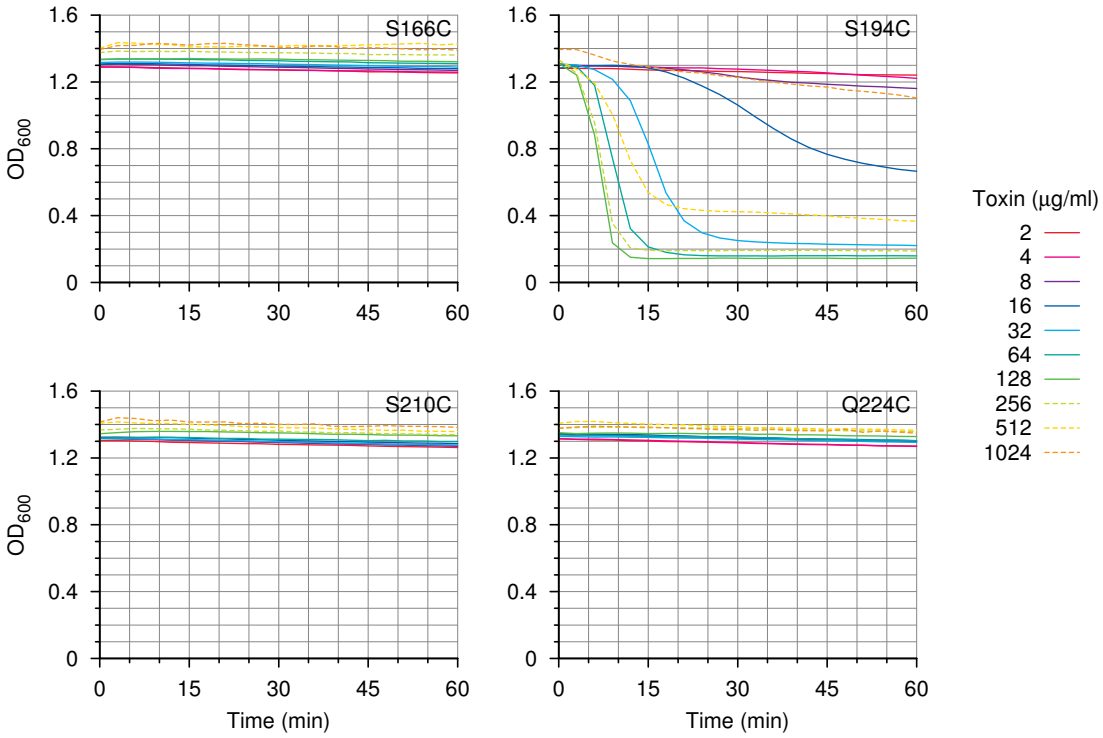

Figure 4.3 Hemolytic activity of the cysteine mutants S166C, S194C, S210C, and Q224C. The mutant proteins, at various final concentrations as indicated, were incubated with red blood cells, and the progress of hemolysis was monitored by the decrease in cell turbidity (OD_{600}).

4.3.2 Hemolytic activities

Figure 4.3 shows the hemolytic activity assays for the mutants S166C, S194C, S210C, and Q224C. The assay format is the same as in Figure 3.1, that is, hemolysis is indicated by a time-dependent decrease in sample turbidity. It is clear that mutants S166C, S210C, and Q224C are devoid of any detectable activity even at very high concentrations.

The only mutant that retains some residual hemolytic activity is S194C. Comparison with the wild-type toxin (see Figure 3.1) indicates that the specific activity of the mutant is reduced by a factor of 8–16. Interestingly, at very high concentrations (>256 µg/mL), the rate of he-

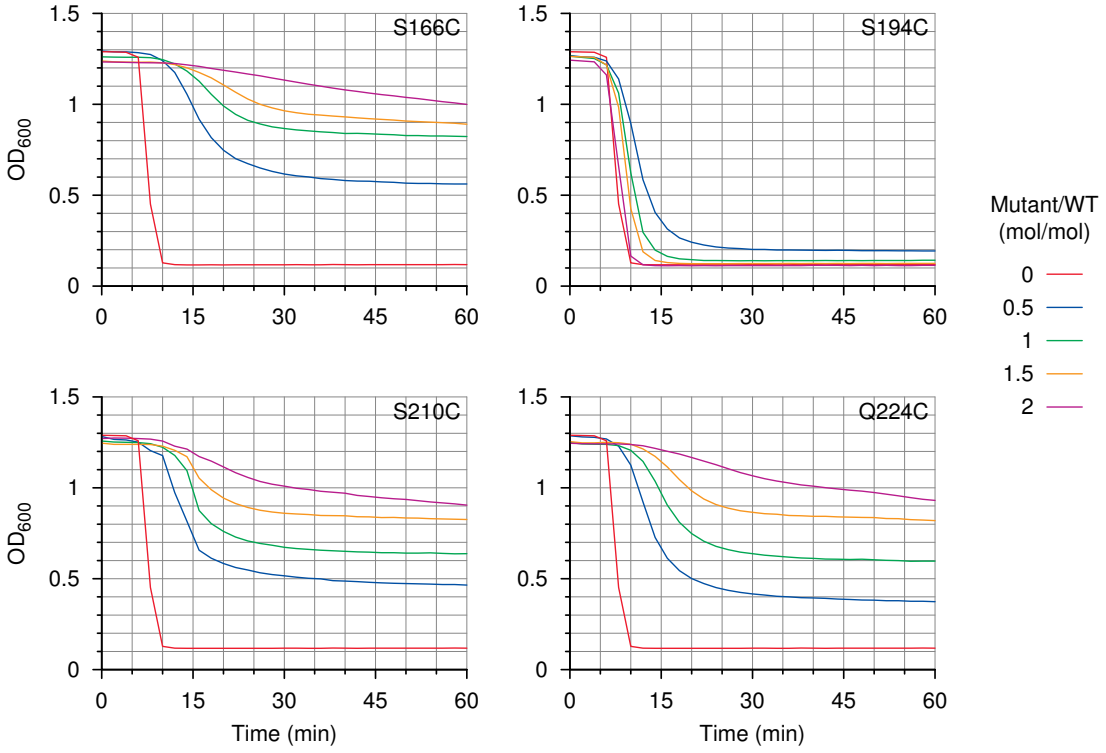

Figure 4.4 Effect of cysteine mutants on the hemolytic activity of wild-type Cyt2Aa1. Wild-type Cyt2Aa1 (16 µg/mL) was supplemented with each cysteine mutant at the molar ratio indicated, and the hemolytic activity of the mixtures was measured using the decrease in cell turbidity (OD_{600}).

molysis drops again, which amounts to a prozone phenomenon similar to that shown in Figure 3.4.

Overall, none of these mutants approach the activity of wild-type toxin or of the previously characterized mutant V186C [110], and so they are not good models of the wild-type toxin. Considering the conservative nature of these mutations, this outcome is surprising.

4.3.3 The interaction of inactive cysteine mutants with wild-type Cyt2Aa1

In both hypothetical action mechanisms of Cyt2Aa1—namely, discrete pore-formation and the detergent-like effect—membrane damage comes

about through a cooperative action of multiple Cyt2Aa1 molecules. The question therefore arises if and how the mutant proteins might interact with wild-type toxin. In an initial experiment, a fixed amount of wild-type Cyt2Aa1 was mixed with the mutant proteins at different molar ratios, and the hemolytic activities of the mixtures were measured (see Figure 4.4). The three mutants with no residual intrinsic activity—that is, S166C, S210C, and Q224C—inhibited the activity of wild-type toxin progressively in a dose-dependent manner. Low concentrations of S194C also displayed a slight degree of inhibition, but the activity increased again at higher proportions of the mutant.

4.3.4 Inhibition by S166C, S210C, and Q224C is not due to competition for binding sites

The inhibition imposed on wild-type Cyt2Aa1 by the three inactive mutants might arise at different stages of the cytolytic action mechanism. The first of these stages consists in the binding of the monomeric toxin molecules to the membrane.

It has been shown previously that Cyt2Aa1 can bind tightly to membranes at low temperatures, but that under these conditions no oligomer formation occurs [110]. We made use of this observation to determine whether the inactive mutants exercise their inhibitory effect during membrane binding or at a later stage. With each mutant, two parallel samples were prepared. Either the wild-type toxin or the mutant was preincubated alone with red blood cells at 4°C. The other protein was then added, and after a second incubation step at 4°C, the sample was transferred to 37°C to initiate hemolysis, the time course of which was recorded.

If the inhibition imposed by the inactive mutants were due to competition for binding sites, then the samples exposed to wild-type toxin first should be exempt from inhibition, since in these samples the active species could occupy all binding sites before addition of the inhibitory ones. On the other hand, addition of the mutants before the wild-

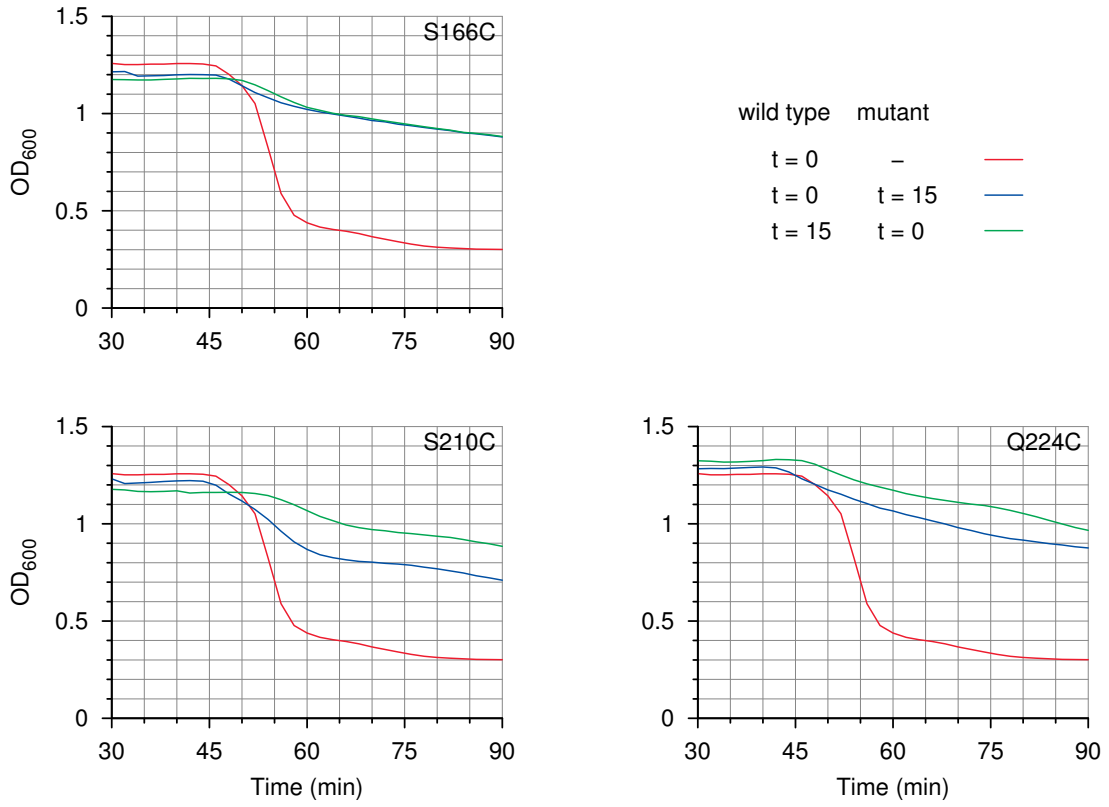

Figure 4.5 Temperature shift experiments to determine the mode of inhibition by inactive cysteine mutants. Wild-type Cyt2Aa1 (16 µg/mL) and the mutant in question (32 µg/mL) were added alone or sequentially at 0 or 15 minutes to red blood cells and incubated at 4°C. After 30 minutes overall, the samples were transferred to 37°C, and the time course of hemolysis observed using the decrease in OD_{600}. Reversing the order of addition has little effect on the extent of inhibition.

type toxin should increase the extent of inhibition, since the wild-toxin would find the available binding sites already occupied.

Figure 4.5 shows that the degree of inhibition was very similar with both types of samples; the rates of hemolysis of the samples exposed to wild-type toxin first were only slightly higher than those preincubated first with the mutants. In all cases, the extent of inhibition was similar to that observed with samples in which the two protein species

had been mixed before addition to the cells (cf. Figure 4.4). From this, it can be concluded that the inhibitory effect of these mutants arises primarily downstream of membrane binding, most likely through some non-productive mutual interaction between wild-type and mutant toxin molecules.

4.3.5 Interaction of wild-type Cyt2Aa1 and S194C

The mutants S166C, S210C and Q224C are inactive, and their inhibitory effects on wild-type toxin may be expected. In contrast, mutant S194C retains partial activity, and its inhibitory effect on wild-type toxin is small or negligible, depending on the molar ratio (cf. Figure 4.4). One might therefore wonder if the interaction between the two species always results in inhibition of the wild-type, or if the latter may be able to rescue the activity of the latter.

Figure 4.6 shows an experiment designed to detect such a possible transactivation of the mutant by wild-type Cyt2Aa1. In panel A, the activity of S194C alone is measured at low concentrations. At 8 µg/mL and below, hemolytic activity is virtually absent. Panel B shows the behaviour of wild-type toxin at 1 µg/mL, combined with different concentrations of S194C. At 1 and 2 µg/mL, the mutant inhibits the activity of the wild-type toxin. Higher, but still non-lytic amounts (4 or 8 µg/mL) of the mutant produce an earlier onset of hemolysis than observed with the same amount of wild-type toxin alone. Thus, the activity of the wild-type toxin is measurably amplified by the addition of mutant toxin, at an amount that on its own lacks detectable activity. This suggests that the wild-type Cyt2Aa1 can recruit some of the mutant molecules into hybrid active oligomers. However, the effect is not large and is observed only in a narrow concentration range. In sum, it appears that, to a very limited degree, wild-type toxin can rescue the activity of the S194C in hybrid supramolecular assemblies.

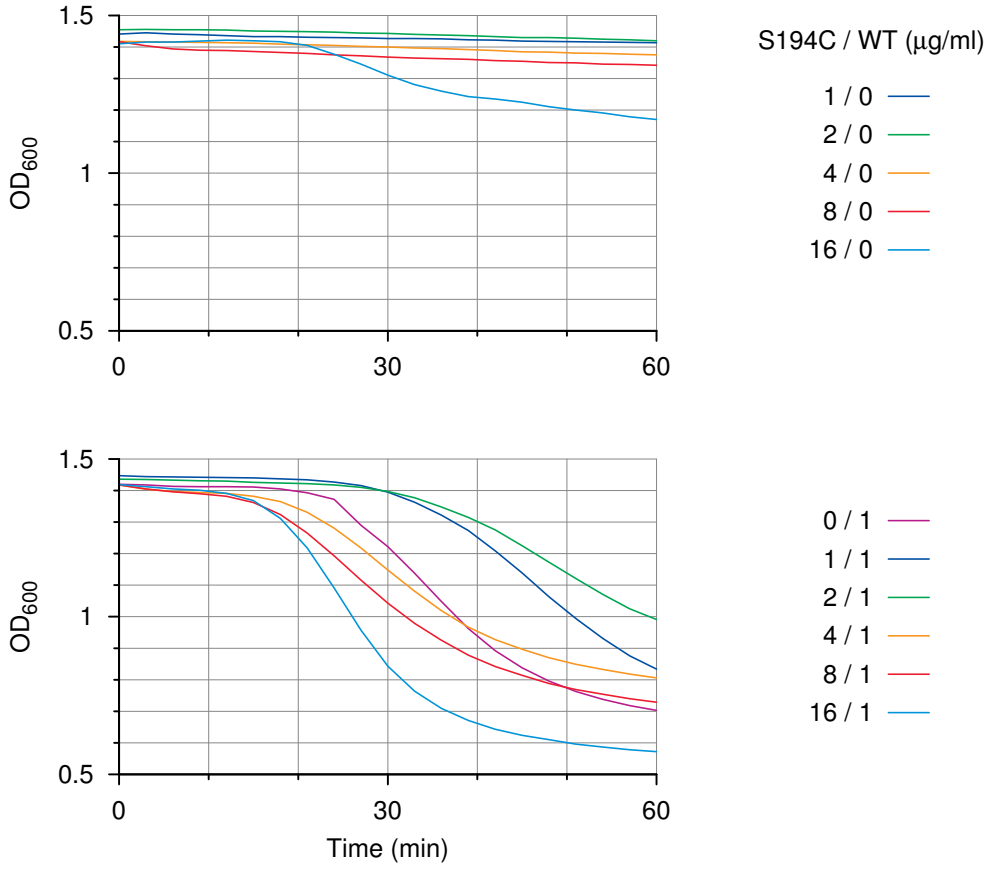

Figure 4.6 Interaction of S194C and wild-type Cyt2Aa1. A: Time course of hemolysis of S194C alone, at various concentrations. B: Time course of hemolysis of the same concentrations of S194C as in A, supplemented with 1 µg/mL of wild-type Cyt2Aa1.

4.3.6 The size of the functional membrane lesion

It has been discussed before that both a detergent-like mechanism and the formation of discrete pores have been proposed to explain the membrane-damaging activity of Cyt2Aa1. With a detergent-like mechanism, the target membrane should disintegrate, and the permeability barrier for solutes of all sizes should break down (cf. Figure 1.3B). On the other

hand, discrete pores would have a finite size and thus should exclude solutes beyond a certain molecular weight.

One experimental approach to detect pores of limited size consists in osmotic protection from hemolysis. An osmolyte of a certain molecular size is added to the cell suspension before the cells are exposed to the pore-forming agent. If the osmolyte is able to traverse the pores, it will equilibrate between the extra-cellular and the intracellular space and thus not balance the excess osmotic activity of hemoglobin; therefore, the cells will undergo lysis. On the other hand, if the osmolyte is too large to traverse the pores, it will be excluded from the intracellular space and maintain the osmotic balance to hemoglobin, thereby preventing hemolysis.

Figure 4.7 shows the effect of the osmolyte polyethyleneglycol (PEG) 1000, which has an effective molecular radius of approximately 1 nm [111], on the time course of hemolysis by wild-type Cyt2Aa1.

It is evident that PEG 1000 delays hemolysis, but does not entirely prevent it. Moreover, the effect varies with the Cyt2Aa1 concentration. With Cyt2Aa1 at 1.5 µg/mL, the presence of PEG 1000 causes a fairly pronounced delay of hemolysis, and the curve deviates from the sigmoidal shape observed without PEG. Increasing the toxin dosage further reduces the delay of hemolysis imposed by PEG.

A possible interpretation for the partial inhibition of hemolysis imposed by PEG is that the toxin indeed forms discrete pores, but that these are heterogeneous in size. If this is the case, pore size might increase with toxin concentration, which could account for the reduced inhibitory effect of PEG.

While many pore-forming toxins form oligomers of uniform subunit stoichiometry and functional diameter, there are exceptions to this rule, including streptolysin O (see [108] and references therein) as well as *Streptococcus agalactiae* CAMP factor [112].

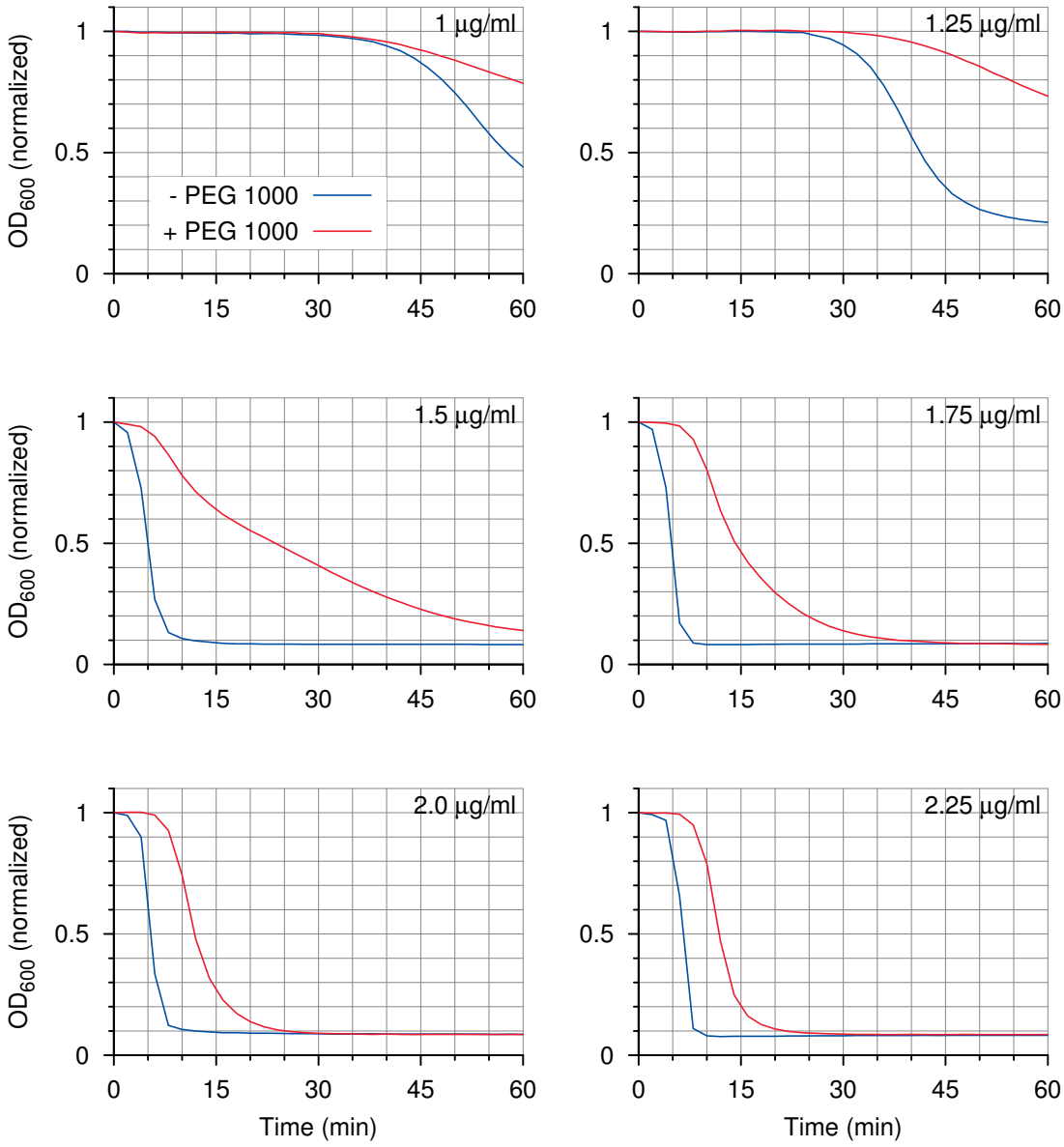

Figure 4.7 Hemolysis kinetics of wild-type Cyt2Aa1 in the absence and presence of PEG 1000 at 10% (v/v). The toxin was used at different final concentrations as indicated in each panel. OD_{600} traces were normalized to t=0, since the raw values were approximately 20% lower with than without PEG, most likely due to the effect of PEG on the refractory index of the solution.

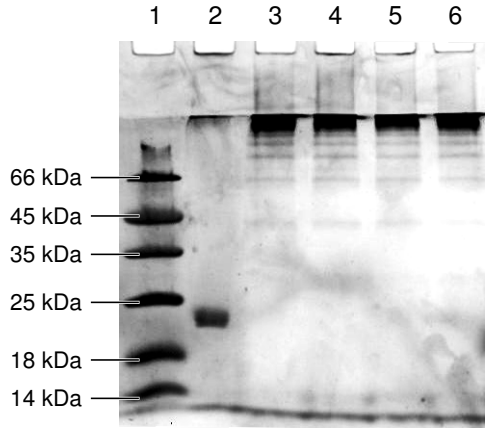

Sample	PC	PG	Cholesterol
2	–	–	–
3	90%	10%	0%
4	85%	5%	10%
5	75%	5%	20%
6	65%	5%	30%

Figure 4.8 SDS-PAGE of Cyt2Aa1 after incubation with liposomes. Activated Cyt2Aa1 (150µg) was incubated without (2) or with (3–6) liposomes (150µg total lipid, molar composition as indicated). The samples were incubated at 37℃ for 2 hours, solubilized with 1% SDS before SDS-PAGE. Lane 1 shows a molecular weight standard.

4.3.7 Cyt2Aa1 forms SDS-resistant oligomers on sensitive and resistant liposome membranes

With many pore-forming toxins, the oligomers that form upon interaction with membranes are stable in the presence of non-denaturing detergents; and some oligomers, such as staphylococcal α-toxin and anthrax toxin protective antigen, also resist dissociation by SDS [64, 113].

Promdonkoy and Ellar have previously used SDS-PAGE followed by Western blotting to characterize the oligomeric state of Cyt2Aa1 after incubation with erythrocyte membranes [110]. They observed the toxin in heterogeneous states of aggregation. We here carried out a similar experiment, using SDS-PAGE on Cyt2Aa1 samples that had been incubated with liposome membranes (since these membranes are free of other proteins, it is possible to use simple protein staining for detection). Figure 4.8A shows that contact of the toxin with liposome membranes transforms it to a variety of higher molecular weight species.

While several distinct bands are visible, most of the protein barely enters the resolving gel and remains unresolved.

The fact that the Cyt2Aa1 oligomers persist upon exposure to SDS implies that the monomers contained within them are not denatured, and therefore that the molecular weights suggested by comparison to the molecular weight marker cannot be taken at face value. Still, the pattern of the observed bands suggests the formation of oligomers of different sizes. If we assume that neighbouring bands differ by one subunit, it would appear that most oligomers possess six or more subunits. This pattern resembles that observed previously observed by Promdonkoy and Ellar on red blood cells, except that higher molecular weights appear to be more prominent on liposomes, and it appears to agree with the possibility of pores with different functional sizes suggested by the osmotic protection experiments.

Another interesting observation is that oligomerization occurs on all tested liposomes, regardless of cholesterol content and susceptibility to permeabilization by Cyt2Aa1 (cf. Section 3.3.4).

4.4 DISCUSSION

As stated at the beginning of this chapter, the intended purpose of the cysteine mutants characterized here was to obtain fluorescently labelled, functionally active derivatives of Cyt2Aa1 that could then be used as probes to study the toxin's interaction with membranes. The finding that none of these mutants were fully active even in unmodified form, and that three out of four were entirely inactive, was unexpected, the more so when considering mutating a serine residue to cysteine amounts to no more than the replacement of a single oxygen atom with sulphur. That these minimal structural changes would result in such pronounced functional responses provides yet another argument against a detergent-like mechanism of membrane damage. Detergent-like properties depend on overall molecular shape and hy-

drophilic-lipophilic balance; small changes to a detergent molecule may modify micelle size or critical micellar concentration, but would not be expected to wholly disrupt the activity. In contrast, the strong functional effects of minor structural changes observed here suggest highly specific molecular interactions.

If we accept that Cyt2Aa1 forms discrete oligomeric pores, then the question arises how many subunits may be contained in each oligomer. Previous studies have provided estimates of six [43] and sixteen [67] subunits. Our current results do not provide a definite number, although they suggest that an oligomer can contain more than six subunits. They also suggest the existence of heterogeneous oligomers. Such heterogeneity has been demonstrated with other pore-forming toxins, including *Streptococcus agalactiae* CAMP factor [112] and *Streptococcus pyogenes* streptolysin O. With the latter toxin, pores can be formed even when the oligomers do not form complete rings but incomplete arc-shaped assemblies [108]. Whether or not this applies to Cyt2Aa1 also might possibly be determined using morphological techniques, particularly electron microscopy, which has proven useful with many different pore-forming proteins.

The observation of oligomers on both susceptible and resistant liposome membranes indicates that oligomerization can occur in the absence of membrane permeabilization. With many pore-forming toxins, it has been shown that oligomerization precedes membrane insertion and permeabilization. Inactive "pre-pore" oligomers have been observed on resistant cell types, for example with α-toxin on granulocytes [114] and with streptolysin O on rodent erythrocytes [115]. Our results thus suggest that Cyt2Aa1 resembles these toxin with respect to the sequence of oligomer formation and membrane insertion. Further analogies are provided by the behaviour of mutant S194C, the transactivation of which by the wild-type toxin resembles that of an insertion mutant of α-toxin [116], and by the dominant-negative phenotypes of the other three cysteine mutants, which resemble those of various α-

toxin [96] and streptolysin O [108] mutants. Overall, our study thus reinforces the notion that Cyt2Aa1 functionally resembles other well-characterized pore-forming toxins.

Chapter 5

Summary and future work

5.1 SUMMARY

This thesis has addressed a number of questions that concern the mode of action and the specificity of *B. thuringiensis* Cyt2Aa1 toxin. In Chapter 2, it was shown that Cyt2Aa1 permeabilizes the membranes of Gram-positive bacteria. The level of activity was found to be considerably lower than that of the homologous Cyt1Aa1 toxin family, and at the attainable toxin concentrations, Gram-negative bacteria were not affected. This is consistent with the finding that Cyt2Aa1, but not Cyt1Aa1 can be expressed in the absence of any inhibitory proteins within *E. coli* cells. The molecular features that cause such a pronounced difference in activity remain to be established.

In contrast to mammalian cell membranes, bacterial membranes do not contain cholesterol. The sterol is known to activate several different families of pore-forming toxins, and therefore the observed low susceptibility of bacterial membranes suggested that Cyt2Aa1 might also be cholesterol-dependent. This hypothesis was tested in Chapter 3 and

rejected, as the sterol was found to inhibit Cyt2Aa1 rather than to activate it. This effect was more clearly evident with synthetic liposomes than with partially cholesterol-depleted red blood cells. The liposome experiments provide simple models for both resistant and susceptible membranes, which may be of use in future reconstitution studies to identify and characterize natural membrane molecules that augment or inhibit the activity of Cyt2Aa1.

Previous studies had proposed two alternative modes of action for Cyt2Aa1, namely, the formation of discrete pores on the one hand, and a detergent-like mechanism on the other. In Chapter 4 of this thesis, we undertook some experiments to shed light on this question. On the whole, our findings support pore-formation rather than a detergent-like mode of action. The toxin does form oligomers upon contact with membranes, which are stable to dissociation with SDS and also appear to be heterogeneous in subunit stoichiometry. This appears to agree with the partial osmotic protection observed with PEG 1000.

5.2 FUTURE WORK

While the studies on different natural and model membranes presented here show substantial differences in susceptibility to Cyt2Aa1, it is still unclear which individual membrane constituents—lipids or proteins—or physical properties determine Cyt2Aa1 activity on membranes. It will be worthwhile to try to identify these determinants. Chemical or enzymatic treatment of membranes to modify phospholipids, glycolipids, or glycoproteins might provide preliminary clues. For definite identification, sensitive membranes, such as those of red blood cells, could be fractionated, and individual membrane lipids or proteins reconstituted into model liposomes in order to determine their effect on Cyt2Aa1 activity.

While Chapter 4 tentatively supports the notion that Cyt2Aa1 forms pores of discrete sizes, with a functional diameter of approximately 2

nm but possibly heterogeneous, this hypothesis should be tested more rigorously using morphological methods. Pores with a diameter on the order of 2 nm should be readily visible by electron microscopy, as has been demonstrated for example with staphylococcal α-toxin [64]. Such studies could help to determine if the size and, potentially, the shape of the membrane lesions are indeed heterogeneous. It may also be possible to observe the structure of the oligomer at higher resolution using cryo-EM. This approach has been very successful with the thiol-activated toxin pneumolysin [117], which, like streptolysin O, forms heterogeneous oligomers that are not amenable to X-ray crystallography.

With many pore-forming toxins, a useful approach to studying the structure-function relationships has been the introduction of single mutant cysteines, which can then be labelled with environmentally sensitive fluorescent dyes. With Cyt2Aa1, only one such study has been published, and this study reported the characterization of only a small number of mutants [110]. In Chapter 4, it was shown that several new cysteine mutants had low or entirely lacking hemolytic activity, which makes them unsuitable as models of the wild-type toxin. Additional mutations should be examined in order to identify functional domains involved in membrane binding and insertion, as well as in the oligomerization of the toxin.

Bibliography

[1] H. T. Dulmage and K. Aizawa: Distribution of *Bacillus subtilis* in nature. In: *Microbial and viral pesticides*. Ed. by E. Kurstak. Marcel Dekker, 1982. Chap. 00, 209–237.

[2] E. Berliner: Über die Schlafsucht der Mehlmottenraupe (*Ephestia kuehniella*) und ihren Erreger, *Bacillus thuringiensis* n.sp. *Z angew Entomol* 2 (1915), 29–56.

[3] C. L. Hannay and P. Fitz-James: The protein crystals of *Bacillus thuringiensis* Berliner. *Can J Microbiol* 1 (1955), 694–710. PMID: 13270146.

[4] K. van Frankenhuyzen: The challenge of *Bacillus thuringiensis*. In: *Bacillus thuringiensis, an environmental biopesticide: theory and practice*. Ed. by P. E. Entwistle, J. S. Cory, M. J. Bailey, and S. Higgs. John Wiley and Sons, 1993, 1–35.

[5] V. Sanchis: From microbial sprays to insect-resistant transgenic plants: history of the biospesticide *Bacillus thuringiensis*. *Agron Sustain Dev* 31 (2011), 317–231. URL: http://doi.org/10.1051/agro/2010027.

[6] G. A. Kleter, R. Bhula, K. Bodnaruk, E. Carazo, A. S. Felsot, C. A. Harris, A. Katayama, H. A. Kuiper, K. D. Racke, B. Rubin, Y. Shevah, G. R. Stephenson, K. Tanaka, J. Unsworth, R. D. Wauchope, and S.-S. Wong: Altered pesticide use on transgenic crops and the associated general impact from an environmental perspective. *Pest Manag Sci* 63 (2007), 1107–1115. PMID: 17880042.

[7] P. A. Martin and R. S. Travers: Worldwide Abundance and Distribution of *Bacillus thuringiensis* Isolates. *Appl Environ Microbiol* 55 (1989), 2437–2442. PMID: 16348022.

[8] H. de Barjec and F. Lemille: Presence of flagellar antigenic subfactors in serotype 3 of *Bacillus thuringiensis*. *J Invertebr Pathol* 15 (1970), 139–140. PMID: 5442846.

[9] K. Aizawa and S. Iida: Nucleic acids extracted from the virus polyhedra of the silkworm *Bombyx mori Linnaeus*. *J Insect Pathol* 5 (1963), 344–348.

[10] R. I. Rautenshtein, L. N. Moskalenko, I. A. Bespalova, and A. S. Tikhonenko: Ultrastructure of bacteriophages specific for *Bacillus thuringiensis* var. galleriae. *Mikrobiologiia* 45 (1976), 690–694. PMID: 979688.

[11] L. J. Goldberg and J. Margalit: A bacterial spore demonstrating rapid larvicidal activity against *Anopheles sergentii*, *Uranotaenia unguiculata*, *Culex univeritattus*, *Aedes aegypti*, and *Culex pipiens*. *Mosquito News* 37 (1977), 355–358.

[12] V. I. Kriukov, V. P. Khodyrev, O. N. Iaroslavtseva, A. S. Kamenova, B. A. Duisembekov, and V. V. Glupov: [Synergistic action of entomopathogenic hyphomycetes and the bacteria *Bacillus thuringiensis* ssp. morrisoni in the infection of Colorado potato beetle *Leptinotarsa decemlineata*]. *Prikl Biokhim Mikrobiol* 45 (2009), 571–576. PMID: 19845290.

[13] M. M. Lecadet, M. O. Blondel, and J. Ribier: Generalized transduction in *Bacillus thuringiensis* var. berliner 1715 using bacteriophage CP-54Ber. *J Gen Microbiol* 121 (1980), 203–212. PMID: 7252480.

[14] M. M. Lecadet, E. Frachon, V. C. Dumanoir, H. Ripouteau, S. Hamon, P. Laurent, and I. Thiéry: Updating the H-antigen classification of *Bacillus thuringiensis*. *J Appl Microbiol* 86 (1999), 660–672. PMID: 10212410.

[15] D. Xu and J.-C. Côté: Sequence diversity of *Bacillus thuringiensis* flagellin (H antigen) protein at the intra-H serotype level. *Appl Environ Microbiol* 74 (2008), 5524–5532. PMID: 18586969.

[16] B. Soufiane and J.-C. Côté: Discrimination among *Bacillus thuringiensis* H serotypes, serovars and strains based on 16S rRNA, gyrB and aroE gene sequence analyses. *Antonie Van Leeuwenhoek* 95 (2009), 33–45. PMID: 18839329.

[17] E. Helgason, O. A. Okstad, D. A. Caugant, H. A. Johansen, A. Fouet, M. Mock, I. Hegna, and A. B. Kolstø: Bacillus anthracis, *Bacillus cereus*, and *Bacillus thuringiensis*–one species on the basis of genetic evidence. *Appl Environ Microbiol* 66 (2000), 2627–2630. PMID: 10831447.

[18] D. A. Rasko, M. R. Altherr, C. S. Han, and J. Ravel: Genomics of the *Bacillus cereus* group of organisms. *FEMS Microbiol Rev* 29 (2005), 303–329. PMID: 15808746.

[19] D. B. Bechtel and L. A. J. Bulla: Electron microscope study of sporulation and parasporal crystal formation in *Bacillus thuringiensis*. *J Bacteriol* 127 (1976), 1472–1481. PMID: 182671.

[20] M. A. Berbert-Molina, A. M. R. Prata, L. G. Pessanha, and M. M. Silveira: Kinetics of *Bacillus thuringiensis* var. *israelensis* growth on high glucose concentrations. *J Ind Microbiol Biotechnol* 35 (2008), 1397–1404. PMID: 18712542.

[21] D. W. Hilbert and P. J. Piggot: Compartmentalization of gene expression during *Bacillus subtilis* spore formation. *Microbiol Mol Biol Rev* 68 (2004), 234–262. PMID: 15187183.

[22] L. Palma, D. Muñoz, C. Berry, J. Murillo, and P. Caballero: Bacillus thuringiensis toxins: an overview of their biocidal activity. *Toxins (Basel)* 6 (2014), 3296–3325. PMID: 25514092.

[23] N. Crickmore, D. R. Zeigler, J. Feitelson, E. Schnepf, J. Van Rie, D. Lereclus, J. Baum, and D. H. Dean: Revision of the nomenclature for the *Bacillus thuringiensis* pesticidal crystal proteins. *Microbiol Mol Biol Rev* 62 (1998), 807–813. PMID: 9729610.

[24] T. Yamamoto and T. Iizuka: Two types of entomocidal toxins in the parasporal crystals of Bacillus thuringiensis kurstaki. *Arch Biochem Biophys* 227 (1983), 233–241. PMID: 6357098.

[25] A. Bravo, M. Soberón, and S. S. Gill: *Bacillus thuringiensis*: Mechanisms and Use. In: *Comprehensive Molecular Insect Science*. Ed. by L. I. Gilbert, K. Iatrou, and S. S. Gill. Vol. 6. Elsevier, 2005. Chap. 6, 175–205.

[26] W. E. Thomas and D. J. Ellar: *Bacillus thuringiensis* var *israelensis* crystal δ-endotoxin: effects on insect and mammalian cells in vitro and in vivo. *J Cell Sci* 60 (1983), 181–197. PMID: 6874728.

[27] C. Zhong, D. J. Ellar, A. Bishop, C. Johnson, S. Lin, and E. R. Hart: Characterization of a *Bacillus thuringiensis* δ-endotoxin which is toxic to insects in three orders. *J Invertebr Pathol* 76 (2000), 131–139. PMID: 11023737.

[28] R. A. de Maagd, A. Bravo, and N. Crickmore: How *Bacillus thuringiensis* has evolved specific toxins to colonize the insect world. *Trends Genet* 17 (2001), 193–199. PMID: 11275324.

[29] Y. Shai: Mode of action of membrane active antimicrobial peptides. *Biopolymers* 66 (2002), 236–248. PMID: 12491537.

[30] M. W. Parker and S. C. Feil: Pore-forming protein toxins: from structure to function. *Prog Biophys Mol Biol* 88 (2005), 91–142. PMID: 15561302.

[31] M. R. Gonzalez, M. Bischofberger, L. Pernot, F. G. van der Goot, and B. Frêche: Bacterial pore-forming toxins: the (w)hole story? *Cell Mol Life Sci* 65 (2008), 493–507. PMID: 17989920.

[32] M. Palmer: Cholesterol and the activity of bacterial toxins. *FEMS Microbiol Lett* 238 (2004), 281–289. PMID: 15358412.

[33] A. Valeva, N. Hellmann, I. Walev, D. Strand, M. Plate, F. Boukhallouk, A. Brack, K. Hanada, H. Decker, and S. Bhakdi: Evidence that clustered phosphocholine head groups serve as sites for binding and assembly of an oligomeric protein pore. *J Biol Chem* 281 (2006), 26014–26021. PMID: 16829693.

[34] L. Eidels, R. L. Proia, and D. A. Hart: Membrane receptors for bacterial toxins. *Microbiol Rev* 47 (1983), 596–620. PMID: 6363900.

[35] K. L. Nelson, S. M. Raja, and J. T. Buckley: The glycosylphosphatidylinositol-anchored surface glycoprotein Thy-1 is a receptor for the channel-forming toxin aerolysin. *J Biol Chem* 272 (1997), 12170–12174. PMID: 9115289.

[36] S. Lang, J. Xue, Z. Guo, and M. Palmer: *Streptococcus agalactiae* CAMP factor binds to GPI-anchored proteins. *Med Microbiol Immunol* 196 (2007), 1–10. PMID: 16773378.

[37] M. Wiener, D. Freymann, P. Ghosh, and R. M. Stroud: Crystal structure of colicin Ia. *Nature* 385 (1997), 461–464. PMID: 9009197.

[38] S. K. Buchanan, P. Lukacik, S. Grizot, R. Ghirlando, M. M. U. Ali, T. J. Barnard, K. S. Jakes, P. K. Kienker, and L. Esser: Structure of colicin I receptor bound to the R-domain of colicin Ia: implications for protein import. *EMBO J* 26 (2007), 2594–2604. PMID: 17464289.

[39] J. E. Wedekind, C. B. Trame, M. Dorywalska, P. Koehl, T. M. Raschke, M. McKee, D. FitzGerald, R. J. Collier, and D. B. McKay: Refined crystallographic structure of *Pseudomonas aeruginosa* exotoxin A and its implications for the molecular

mechanism of toxicity. *J Mol Biol* 314 (2001), 823–837. PMID: 11734000.

[40] N. Galitsky, V. Cody, A. Wojtczak, D. Ghosh, J. R. Luft, W. Pangborn, and L. English: Structure of the insecticidal bacterial δ-endotoxin Cry3Bb1 of *Bacillus thuringiensis*. *Acta Crystallogr D Biol Crystallogr* 57 (2001), 1101–1109. PMID: 11468393.

[41] L. Song, M. R. Hobaugh, C. Shustak, S. Cheley, H. Bayley, and J. E. Gouaux: Structure of staphylococcal α-hemolysin, a heptameric transmembrane pore. *Science* 274 (1996), 1859–1866. PMID: 8943190.

[42] J. Rossjohn, S. C. Feil, W. J. McKinstry, R. K. Tweten, and M. W. Parker: Structure of a cholesterol-binding, thiol-activated cytolysin and a model of its membrane form. *Cell* 89 (1997), 685–692.

[43] J. Li, P. A. Koni, and D. J. Ellar: Structure of the mosquitocidal δ-endotoxin CytB from *Bacillus thuringiensis* sp. *kyushuensis* and implications for membrane pore formation. *J Mol Biol* 257 (1996), 129–152. PMID: 8632451.

[44] H. P. Bietlot, I. Vishnubhatla, P. R. Carey, M. Pozsgay, and H. Kaplan: Characterization of the cysteine residues and disulphide linkages in the protein crystal of *Bacillus thuringiensis*. *Biochem J* 267 (1990), 309–315. PMID: 2110449.

[45] J. D. Li, J. Carroll, and D. J. Ellar: Crystal structure of insecticidal δ-endotoxin from *Bacillus thuringiensis* at 2.5 A resolution. *Nature* 353 (1991), 815–821. PMID: 1658659.

[46] P. A. Koni and D. J. Ellar: Cloning and characterization of a novel *Bacillus thuringiensis* cytolytic δ-endotoxin. *J Mol Biol* 229 (1993), 319–327. PMID: 8429550.

[47] S. S. Gill, E. A. Cowles, and P. V. Pietrantonio: The mode of action of *Bacillus thuringiensis* endotoxins. *Annu Rev Entomol* 37 (1992), 615–636. PMID: 1311541.

[48] A. Bravo, S. S. Gill, and M. Soberón: Mode of action of *Bacillus thuringiensis* Cry and Cyt toxins and their potential for insect control. *Toxicon* 49 (2007), 423–435. PMID: 17198720.

[49] R. A. de Maagd, A. Bravo, C. Berry, N. Crickmore, and H. E. Schnepf: Structure, diversity, and evolution of protein toxins from spore-forming entomopathogenic bacteria. *Annu Rev Genet* 37 (2003), 409–433. PMID: 14616068.

[50] P. Boonserm, P. Davis, D. J. Ellar, and J. Li: Crystal structure of the mosquito-larvicidal toxin Cry4Ba and its biological implications. *J Mol Biol* 348 (2005), 363–382. PMID: 15811374.

[51] R. K. Vadlamudi, E. Weber, I. Ji, T. H. Ji, and L. A. J. Bulla: Cloning and expression of a receptor for an insecticidal toxin of *Bacillus thuringiensis*. *J Biol Chem* 270 (1995), 5490–5494. PMID: 7890666.

[52] J. L. Jurat-Fuentes and M. J. Adang: Characterization of a Cry1Ac-receptor alkaline phosphatase in susceptible and resistant Heliothis virescens larvae. *Eur J Biochem* 271 (2004), 3127–3135. PMID: 15265032.

[53] A. P. Valaitis, J. L. Jenkins, M. K. Lee, D. H. Dean, and K. J. Garner: Isolation and partial characterization of gypsy moth BTR-270, an anionic brush border membrane glycoconjugate that binds *Bacillus thuringiensis* Cry1A toxins with high affinity. *Arch Insect Biochem Physiol* 46 (2001), 186–200. PMID: 11304752.

[54] P. Grochulski, L. Masson, S. Borisova, M. Pusztai-Carey, J. L. Schwartz, R. Brousseau, and M. Cygler: *Bacillus thuringiensis* CryIA(a) insecticidal toxin: crystal structure and channel formation. *J Mol Biol* 254 (1995), 447–464. PMID: 7490762.

[55] R. J. Morse, T. Yamamoto, and R. M. Stroud: Structure of Cry2Aa suggests an unexpected receptor binding epitope. *Structure* 9 (2001), 409–417. PMID: 11377201.

[56] S.-C. Lin, Y.-C. Lo, J.-Y. Lin, and Y.-C. Liaw: Crystal structures and electron micrographs of fungal volvatoxin A2. *J Mol Biol* 343 (2004), 477–491. PMID: 15451675.

[57] P. A. Koni and D. J. Ellar: Biochemical characterization of *Bacillus thuringiensis* cytolytic δ-endotoxins. *Microbiology* 140 (1994), 1869–1880. PMID: 7921240.

[58] A. Hilbeck and J. E. U. Schmidt: Another View on Bt Proteins – How Specific are They and What Else Might They Do? *Biopesticides International* 2 (2006), 1–50. URL: http://goo.gl/CdMzMi.

[59] S. D. Manceva, M. Pusztai-Carey, P. S. Russo, and P. Butko: A detergent-like mechanism of action of the cytolytic toxin Cyt1A from *Bacillus thuringiensis* var. *israelensis*. *Biochemistry* 44 (2005), 589–597. PMID: 15641784.

[60] B. Promdonkoy and D. J. Ellar: Structure-function relationships of a membrane pore forming toxin revealed by reversion mutagenesis. *Mol Membr Biol* 22 (2005), 327–337. PMID: 16154904.

[61] B. Promdonkoy and D. J. Ellar: Membrane pore architecture of a cytolytic toxin from *Bacillus thuringiensis*. *Biochem J* 350 (2000), 275–282. PMID: 10926854.

[62] F. G. Prendergast, M. Meyer, G. L. Carlson, S. Iida, and J. D. Potter: Synthesis, spectral properties, and use of 6-acryloyl-2-dimethylaminonaphthalene (Acrylodan). A thiol-selective, polarity-sensitive fluorescent probe. *J Biol Chem* 258 (1983), 7541–7544. PMID: 6408077.

[63] R. J. Ward, M. Palmer, K. Leonard, and S. Bhakdi: Identification of a putative membrane-inserted segment in the α-toxin of *Staphylococcus aureus*. *Biochemistry* 33 (1994), 7477–7484. PMID: 8003513.

[64] S. Bhakdi, R. Füssle, and J. Tranum-Jensen: Staphylococcal α-toxin: oligomerization of hydrophilic monomers to form amphiphilic hexamers induced through contact with deoxycholate detergent micelles. *Proc Natl Acad Sci U S A* 78 (1981), 5475–5479. PMID: 6272304.

[65] A. Zitzer, I. Walev, M. Palmer, and S. Bhakdi: Characterization of *Vibrio cholerae* El Tor cytolysin as an oligomerizing pore-forming toxin. *Med Microbiol Immunol* 184 (1995), 37–44. PMID: 8538577.

[66] F. A. Drobniewski and D. J. Ellar: Investigation of the membrane-lesion induced in vitro by two mosquitocidal δ-endotoxins of *Bacillus thuringiensis*. *Curr Microbiol* 16 (1988), 195–199. URL: http://dx.doi.org/10.1007/BF01568529.

[67] E. Chow, G. J. Singh, and S. S. Gill: Binding and aggregation of the 25-kilodalton toxin of *Bacillus thuringiensis* subsp. *israelensis* to cell membranes and alteration by monoclonal antibodies and amino acid modifiers. *Appl Environ Microbiol* 55 (1989), 2779–2788. PMID: 2624459.

[68] B. H. Knowles, P. J. White, C. N. Nicholls, and D. J. Ellar: A broad-spectrum cytolytic toxin from *Bacillus thuringiensis* var. *kyushuensis*. *Proc Biol Sci* 248 (1992), 1–7. PMID: 1355907.

[69] P. Butko, F. Huang, M. Pusztai-Carey, and W. K. Surewicz: Membrane permeabilization induced by cytolytic δ-endotoxin CytA from *Bacillus thuringiensis* var. *israelensis*. *Biochemistry* 35 (1996), 11355–11360. PMID: 8784190.

[70] J. Douek, M. Einav, and A. Zaritsky: Sensitivity to plating of *Escherichia coli* cells expressing the cryA gene from *Bacillus thuringiensis* var. *israelensis*. *Mol Gen Genet* 232 (1992), 162–165. PMID: 1313146.

[71] R. Manasherob, A. Zaritsky, E. Ben-Dov, D. Saxena, Z. Barak, and M. Einav: Effect of accessory proteins P19 and P20 on cytolytic activity of Cyt1Aa from Bacillus thuringiensis subsp. israelensis in Escherichia coli. *Curr Microbiol* 43 (2001), 355–364. PMID: 11688801.

[72] T. G. Yudina, A. V. Konukhova, L. P. Revina, L. I. Kostina, I. A. Zalunin, and G. G. Chestukhina: Antibacterial activity of Cry- and Cyt-proteins from *Bacillus thuringiensis* ssp. *israelensis*. *Can J Microbiol* 49 (2003), 37–44. PMID: 12674346.

[73] T. G. Yudina, A. L. Brioukhanov, I. A. Zalunin, L. P. Revina, A. I. Shestakov, N. E. Voyushina, G. G. Chestukhina, and A. I. Netrusov: Antimicrobial activity of different proteins and their fragments from *Bacillus thuringiensis* parasporal crystals against clostridia and archaea. *Anaerobe* 13 (2007), 6–13. PMID: 17126041.

[74] M. Itsko, R. Manasherob, and A. Zaritsky: Partial restoration of antibacterial activity of the protein encoded by a cryptic open reading frame (cyt1Ca) from *Bacillus thuringiensis* subsp. *israelensis* by site-directed mutagenesis. *J Bacteriol* 187 (2005), 6379–6385. PMID: 16159771.

[75] M. Itsko and A. Zaritsky: Exposing cryptic antibacterial activity in Cyt1Ca from *Bacillus thuringiensis israelensis* by genetic manipulations. *FEBS Lett* 581 (2007), 1775–1782. PMID: 17418824.

[76] R. Cahan, H. Friman, and Y. Nitzan: Antibacterial activity of Cyt1Aa from *Bacillus thuringiensis* subsp. *israelensis*. *Microbiology* 154 (2008), 3529–3536. PMID: 18957605.

[77] J. J. Estruch, G. W. Warren, M. A. Mullins, G. J. Nye, J. A. Craig, and M. G. Koziel: Vip3A, a novel *Bacillus thuringiensis* vegetative insecticidal protein with a wide spectrum of activities against lepidopteran insects. *Proc Natl Acad Sci U S A* 93 (1996), 5389–5394. PMID: 8643585.

[78] E. Mizuki, Y. S. Park, H. Saitoh, S. Yamashita, T. Akao, K. Higuchi, and M. Ohba: Parasporin, a human leukemic cell-recognizing parasporal protein of *Bacillus thuringiensis*. *Clin Diagn Lab Immunol* 7 (2000), 625–634. PMID: 10882663.

[79] T. Akiba, K. Higuchi, E. Mizuki, K. Ekino, T. Shin, M. Ohba, R. Kanai, and K. Harata: Nontoxic crystal protein from *Bacillus thuringiensis* demonstrates a remarkable structural similarity to β-pore-forming toxins. *Proteins* 63 (2006), 243–248. PMID: 16400649.

[80] E. Mizuki, M. Ohba, T. Akao, S. Yamashita, H. Saitoh, and Y. S. Park: Unique activity associated with non-insecticidal *Bacillus thuringiensis* parasporal inclusions: in vitro cell-killing action on human cancer cells. *J Appl Microbiol* 86 (1999), 477–486. PMID: 10196753.

[81] D. W. Lee, T. Akao, S. Yamashita, H. Katayama, M. Maeda, H. Saitoh, E. Mizuki, and M. Ohba: Noninsecticidal parasporal proteins of a *Bacillus thuringiensis* serovar shandongiensis isolate exhibit a preferential cytotoxicity against human leukemic T cells. *Biochem Biophys Res Commun* 272 (2000), 218–223. PMID: 10872830.

[82] M. S. A. Rahman: Cloning and expression of Cyt2Aa1 toxin and characterization of its mode of action. Master's thesis. University of Waterloo, 2010. URL: https://uwspace.uwaterloo.ca/bitstream/handle/10012/5185/AbdelRahman_Mohamed.pdf.

[83] J. W. Dubendorff and F. W. Studier: Controlling basal expression in an inducible T7 expression system by blocking the target T7 promoter with lac repressor. *J Mol Biol* 219 (1991), 45–59. PMID: 1902522.

[84] R. N. Ramanan, B. T. T. Tey, T. C. Ling, and A. B. Ariff: Classification of pressure range based on the characterization of *Escherichia coli* cell disruption in a high pressure homogenizer. *Am J Biochem Biotech* 5 (2009), 21–29.

[85] J. Li, P. A. Koni, and D. J. Ellar: Crystallization of a membrane pore-forming protein with mosquitocidal activity from *Bacillus thuringiensis* subspecies *kyushuensis*. *Proteins* 23 (1995), 290–293. PMID: 8592711.

[86] X. Luo, L. Chen, Q. Huang, J. Zheng, W. Zhou, D. Peng, L. Ruan, and M. Sun: *Bacillus thuringiensis* metalloproteinase Bmp1 functions as a nematicidal virulence factor. *Appl Environ Microbiol* 79 (2013), 460–468. PMID: 23124228.

[87] S. M. Stocks: Mechanism and use of the commercially available viability stain, BacLight. *Cytometry A* 61 (2004), 189–195. PMID: 15382024.

[88] D. Patel, C. Kosmidis, S. M. Seo, and G. W. Kaatz: Ethidium bromide MIC screening for enhanced efflux pump gene expression or efflux activity in Staphylococcus aureus. *Antimicrob Agents Chemother* 54 (2010), 5070–5073. PMID: 20855743.

[89] R. B. Clayton: The utilization of sterols by insects. *J Lipid Res* 5 (1964), 3–19. PMID: 14173327.

[90] S. Parathath, M. A. Connelly, R. A. Rieger, S. M. Klein, N. A. Abumrad, M. De La Llera-Moya, C. R. Iden, G. H. Rothblat, and D. L. Williams: Changes in plasma membrane properties and phosphatidylcholine subspecies of insect Sf9 cells due to expres-

sion of scavenger receptor class B, type I, and CD36. *J Biol Chem* 279 (2004), 41310–41318. PMID: 15280390.

[91] Y. Ohtani, T. Irie, K. Uekama, K. Fukunaga, and J. Pitha: Differential effects of alpha-, beta- and gamma-cyclodextrins on human erythrocytes. *Eur J Biochem* 186 (1989), 17–22. PMID: 2598927.

[92] R. Zidovetzki and I. Levitan: Use of cyclodextrins to manipulate plasma membrane cholesterol content: evidence, misconceptions and control strategies. *Biochim Biophys Acta* 1768 (2007), 1311–1324. PMID: 17493580.

[93] T. L. Steck, J. Ye, and Y. Lange: Probing red cell membrane cholesterol movement with cyclodextrin. *Biophys J* 83 (2002), 2118–2125. PMID: 12324429.

[94] E. P. Kilsdonk, P. G. Yancey, G. W. Stoudt, F. W. Bangerter, W. J. Johnson, M. C. Phillips, and G. H. Rothblat: Cellular cholesterol efflux mediated by cyclodextrins. *J Biol Chem* 270 (1995), 17250–17256. PMID: 7615524.

[95] R. F. Chen and J. R. Knutson: Mechanism of fluorescence concentration quenching of carboxyfluorescein in liposomes: energy transfer to nonfluorescent dimers. *Anal Biochem* 172 (1988), 61–77. PMID: 3189776.

[96] R. Jursch, A. Hildebrand, G. Hobom, J. Tranum-Jensen, R. Ward, M. Kehoe, and S. Bhakdi: Histidine residues near the N terminus of staphylococcal α-toxin as reporters of regions that are critical for oligomerization and pore formation. *Infect Immun* 62 (1994), 2249–2256. PMID: 8188346.

[97] N. J. Schmidt and H. B. Harding: The demonstration of substances in human sera which inhibit complement fixation in antigen-antibody systems of lymphogranuloma venereum, psit-

tacosis, mumps, Q fever, and lymphocytic choriomeningitis. *J Bacteriol* 71 (1956), 217–222. PMID: 13295197.

[98] G. J. Nelson: Lipid composition of erythrocytes in various mammalian species. *Biochim Biophys Acta* 144 (1967), 221–232. PMID: 6064604.

[99] B. Ramstedt and J. P. Slotte: Interaction of cholesterol with sphingomyelins and acyl-chain-matched phosphatidylcholines: a comparative study of the effect of the chain length. *Biophys J* 76 (1999), 908–915. PMID: 9929492.

[100] K. Simons and E. Ikonen: Functional rafts in cell membranes. *Nature* 387 (1997), 569–572. PMID: 9177342.

[101] R. Leventis and J. R. Silvius: Use of cyclodextrins to monitor transbilayer movement and differential lipid affinities of cholesterol. *Biophys J* 81 (2001), 2257–2267. PMID: 11566796.

[102] M. Silberkang, C. M. Havel, D. S. Friend, B. J. McCarthy, and J. A. Watson: Isoprene synthesis in isolated embryonic Drosophila cells. I. Sterol-deficient eukaryotic cells. *J Biol Chem* 258 (1983), 8503–8511. PMID: 6863298.

[103] A. K. Dwivedy: Effect of cholesterol deficiency on the composition of phospholipids and fatty acids of the housefly, Musca domestica. *J Insect Physiol* 23 (1977), 549–557. PMID: 903662.

[104] S. Bhakdi and J. Tranum-Jensen: Molecular nature of the complement lesion. *Proc Natl Acad Sci U S A* 75 (1978), 5655–5659. PMID: 281714.

[105] P. Plackett and G. G. Alton: A mechanism for prozone formation in the complement fixation test for bovine brucellosis. *Aust Vet J* 51 (1975), 374–377. PMID: 811200.

[106] J. E. Gouaux, O. Braha, M. R. Hobaugh, L. Song, S. Cheley, C. Shustak, and H. Bayley: Subunit stoichiometry of staphylococcal α-hemolysin in crystals and on membranes: a heptameric transmembrane pore. *Proc Natl Acad Sci U S A* 91 (1994), 12828–12831. PMID: 7809129.

[107] A. Valeva, M. Palmer, K. Hilgert, M. Kehoe, and S. Bhakdi: Correct oligomerization is a prerequisite for insertion of the central molecular domain of staphylococcal α-toxin into the lipid bilayer. *Biochim Biophys Acta* 1236 (1995), 213–218. PMID: 7794960.

[108] M. Palmer, R. Harris, C. Freytag, M. Kehoe, J. Tranum-Jensen, and S. Bhakdi: Assembly mechanism of the oligomeric streptolysin O pore: the early membrane lesion is lined by a free edge of the lipid membrane and is extended gradually during oligomerization. *EMBO J* 17 (1998), 1598–1605. PMID: 9501081.

[109] L. A. Shepard, A. P. Hueck, B. D. Hamman, J. Rossjohn, M. W. Parker, R. K. Ryan, A. E. Johnson, and R. K. Tweten: Perfringolysin O: an α-helical to β-sheet transition identified by fluorescence spectroscopy. *Biochemistry* 37 (1998), 293–299.

[110] B. Promdonkoy and D. J. Ellar: Investigation of the pore-forming mechanism of a cytolytic δ-endotoxin from *Bacillus thuringiensis*. *Biochem J* 374 (2003), 255–259. PMID: 12795638.

[111] R. Scherrer and P. Gerhardt: Molecular sieving by the *Bacillus megaterium* cell wall and protoplast. *J Bacteriol* 107 (1971), 718–735. PMID: 4999413.

[112] S. Lang and M. Palmer: Characterization of *Streptococcus agalactiae* CAMP factor as a pore-forming toxin. *J Biol Chem* 278 (2003), 38167–38173. PMID: 12835325.

[113] J. G. Bann: Anthrax toxin protective antigen–insights into molecular switching from prepore to pore. *Protein Sci* 21 (2012), 1–12. PMID: 22095644.

[114] A. Valeva, I. Walev, M. Pinkernell, B. Walker, H. Bayley, M. Palmer, and S. Bhakdi: Transmembrane β-barrel of staphylococcal α-toxin forms in sensitive but not in resistant cells. *Proc Natl Acad Sci U S A* 94 (1997), 11607–11611. PMID: 9326657.

[115] I. Walev, M. Palmer, A. Valeva, U. Weller, and S. Bhakdi: Binding, oligomerization, and pore formation by streptolysin O in erythrocytes and fibroblast membranes: detection of nonlytic polymers. *Infect Immun* 63 (1995), 1188–1194. PMID: 7890371.

[116] A. Valeva, R. Schnabel, I. Walev, F. Boukhallouk, S. Bhakdi, and M. Palmer: Membrane insertion of the heptameric staphylococcal α-toxin pore. A domino-like structural transition that is allosterically modulated by the target cell membrane. *J Biol Chem* 276 (2001), 14835–14841. PMID: 11279048.

[117] S. J. Tilley, E. V. Orlova, R. J. C. Gilbert, P. W. Andrew, and H. R. Saibil: Structural basis of pore formation by the bacterial toxin pneumolysin. *Cell* 121 (2005), 247–256. PMID: 15851031.